A framework for comparing structural and functional measures of glaucomatous damage

Donald C. Hood[a] and **Randy H. Kardon**[b]

a *Departments of Psychology and Ophthalmology, Columbia University, 116th and Broadway, New York, NY, 10027-7004, USA*

b *Department of Ophthalmology and Visual Sciences, University of Iowa and Veterans Administration, 200 Hawkins Drive (PFP), Iowa City, IA 52242 USA*

Abstract

While it is often said that structural damage due to glaucoma precedes functional damage, it is not always clear what this statement means. This review has two purposes: first, to show that a simple linear relationship describes the data relating a particular functional test (standard automated perimetry (SAP)) to a particular structural test (optical coherence tomography (OCT)); and, second, to propose a general framework for relating structural and functional damage, and for evaluating if one precedes the other. The specific functional and structural tests employed are described in Section 2. To compare SAP sensitivity loss to loss of the retinal nerve fiber layer (RNFL) requires a map that relates local field regions to local regions of the optic disc as described in Section 3. When RNFL thickness in the superior and inferior arcuate sectors of the disc are plotted against SAP sensitivity loss (dB units) in the corresponding arcuate regions of the visual field, RNFL thickness becomes asymptotic for sensitivity losses greater than about 10 dB. These data are well described by a simple linear model presented in Section 4. The model assumes that the RNFL thickness measured with OCT has two components. One component is the axons of the retinal ganglion cells and the other, the residual, is everything else (e.g. glial cells, blood vessels). The axon portion is assumed to decrease in a linear fashion with losses in SAP sensitivity (in linear units); the residual portion is assumed to remain constant. Based upon severe SAP losses in anterior ischemic optic neuropathy (AION), the residual RNFL thickness in the arcuate regions is, on average, about one-third of the premorbid (normal) thickness of that region. The model also predicts that, to a first approximation, SAP sensitivity in control subjects does not depend upon RNFL thickness. The data (Section 6) are, in general, consistent with this prediction showing a very weak correlation between RNFL thickness and SAP sensitivity. In Section 7, the model is used to estimate the proportion of patients showing statistical abnormalities (worse than the 5th percentile) on the OCT RNFL test before they show abnormalities on the 24-2 SAP field test. Ignoring measurement error, the patients with a relatively thick RNFL, when healthy, will be more likely to show significant SAP sensitivity loss before statistically significant OCT RNFL loss, while the reverse will be true for those who start with an average or a relatively thin RNFL when healthy. Thus, it is important to understand the implications of the wide variation in RNFL thickness among control subjects. Section 8 describes two of the factors contributing to this variation, variations in the position of blood vessels and variations in the mapping of field regions to disc sectors. Finally, in Sections 7 and 9, the findings are related to the general debate in the literature about the relationship between structural and functional glaucomatous

Corresponding author. Tel/fax: +1-212-854-4587/3609, E-mail address: dch3@columbia.edu (D.C. Hood).

damage and a framework is proposed for understanding what is meant by the question, 'Does structural damage precede functional damage in glaucoma?' An emphasis is placed upon the need to distinguish between "statistical" and "relational" meanings of this question.

1. Introduction

Glaucoma causes damage to the retinal ganglion cells (RGCs), their axons and associated glial cells. This damage leads to characteristic changes in the appearance of the optic disc (nerve head) and in the patterns of vision loss measured with behavioral techniques (e.g. standard automated perimetry (SAP)). In fact, glaucoma is distinguished from other progressive optic neuropathies by characteristic changes in the structure (e.g. the appearance of cupping of the optic disc) and by a decrease in visual function (e.g. loss of sensitivity to light), primarily outside of the center of the visual field (see for example, Ritch et al, 1996; Weinreb and Anton-Lopez, 1999).

It is safe to say that glaucoma experts agree on three key points. 1) the most important clinical challenges in glaucoma are the detection of early glaucomatous damage and its progression over time; 2) *both* structural and functional tests are important in assessing early damage and progression; and 3) significant RGC damage can occur *before* standard tests detect a functional loss in vision. While the evidence for this last point is controversial (see Section 7.2 for a discussion), it has motivated the development of new structural and functional tests. (For reviews of these structural and functional tests, see, for example, Johnson, 2001; Sample and Johnson, 2001; Chauhan, 2004; Girkin, 2004; Stein et al, 2004; Anderson, 2006; Spaeth et al, 2006; Zangwill and Bowd, 2006.)

Although the glaucoma specialist still depends upon direct fundus examination to assess structural damage of the optic disc, the last ten years has seen the emergence of a variety of new technologies for the objective, and non-invasive, measurement of structural changes secondary to RGC damage. Glaucoma specialists today still rely on visual fields, as measured with standard automated perimetry (see Section 2.1), as the primary functional measure to detect and follow glaucomatous damage. However a variety of other functional tests, both behavioral and electrophysiological, have been used with varying degrees of success.

Among glaucoma specialists there is a lack of agreement on the answers to two key questions. The first question is: How does one assess whether a particular structural or functional test is the most sensitive for detecting early glaucomatous damage and its progression? Currently, a good methodology for a direct comparison of tests is lacking. The problems with the typical sensitivity/specificity analysis are well known. For example, the results are heavily dependent on the definition of glaucoma and the extent of glaucomatous damage in the patients studied. The second question is: What is the relationship between the functional loss in the sensitivity to light and the structural loss of RGC axons? This review addresses these two key questions.

In particular, we examine the relationship between the most common functional test, the 24-2 SAP visual field, and one of the new structural tests of RGC axon loss, retinal nerve fiber (RNFL) thickness measured with optical coherence tomography (OCT). After reviewing these techniques, a simple theoretical relationship is proposed. Using this theoretical relationship, a general framework for relating structural and functional damage is presented. Finally, an approach for assessing whether a particular structural or functional test will be more sensitive in detecting early glaucoma and/or monitoring its progression is presented.

2. The Functional and Structural Measures

2.1 A functional measure: Standard automated perimetry (SAP) and the visual field

The primary functional measure of interest here is the visual field. While a variety of procedures are available for measuring visual fields, all fields discussed here were measured with the 24-2 program (SITA standard) and the Humphrey Visual Field Analyzer (Zeiss Meditec, Dublin, CA). This particular test is a form of standard automated perimetry (SAP) and will be referred to here as the SAP field test and the result as the SAP field. The SAP field test is currently the "clinical standard" for detecting and monitoring glaucomatous functional damage, with millions of SAP fields measured each year. For those readers unfamiliar with the test, the subject's task is to press a button when he or she detects the presence of a small (0.43 degree diameter), brief (200 ms) test light presented on a background (10 candelas/m^2). The patient is asked to maintain the same eye position by fixating on a small centrally located fixation light. The test light is presented randomly to 54 locations within the central 24 degrees (48 degree diameter) of the visual field. These locations are spaced 6 degrees apart. The tester has the option of including a test spot in the center (fovea) bringing the total to 55 locations. Figure 1 shows the test points overlaid on a fundus picture (panel A) of the right eye and on an artist's depiction (panel B) of a fundus view showing the retinal nerve fibers, which are the axons of the RGCs.

An example of a 24-2 SAP field report can be seen in Fig. 2B. These are the results for the right eye of a patient with glaucoma. The upper left panel of Fig. 2B, expanded in Fig. 2A, shows the patient's sensitivity at each point expressed on a dB scale of light attenuation (1 dB=0.1 log unit). For example, the circle indicates a location with a sensitivity of 27 dB. At this location, the standard 10,000 apostilb white light had to be attenuated by 27 dB (2.7 log units or a factor of 501) to reach a threshold level of detection. Figure 2C is called the "Total Deviation" plot. To derive a total deviation value, the sensitivity value for age-matched norms is subtracted from the patient's sensitivity value at each test location. So for the test point illustrated (circled), the normal age-matched population had a sensitivity of 29 dB and thus the total deviation for that location was −2 dB less sensitive (27 dB minus 29 dB). Unless otherwise noted, we will use these total deviation values in our analyses. Thus, it is important to understand what they measure. A total deviation of −10 dB indicates that sensitivity at that location is decreased by 1 log unit, or that sensitivity is a factor of 10 less, compared to that of the average of the age-matched control group, while a −3 dB value indicates sensitivity is decreased by 0.3 log unit or a factor of 2 compared to normal. The lower left panel of Fig. 2B codes these total deviation values in the form of a probability map of the visual field, where the significance level is coded from 5% (square of 4 dots) to 0.5% (filled black square). See Anderson and Patella (1999) and Heijl and Patella (2002) for more details including a description of other aspects of the report in Fig. 2B.

2.2 A structural measure: Optical coherence tomography (OCT) and retinal nerve fiber (RNFL) thickness

The main structural test of interest in this review is the retinal nerve fiber (RNFL) thickness as measured with the Stratus OCT (Carl Zeiss Meditec, Inc., Dublin, California, USA). [Unless otherwise specified, version 4.0 software and the fast scan protocol were used.] However, the analysis that we propose can be easily applied to other measures of optic nerve structure. The OCT technique uses an interferometric method to obtain the depth of surfaces differing in reflectance much in the way sonar or ultrasound works (Huang et al., 1991; Schuman et al., 1995). This technique has been reviewed previously in this journal (Costa et al., 2006; van Velthoven et al., 2007; see also Schuman et al., 2004). Briefly, the OCT technique is based upon a comparison of the coherence between two near-infrared laser lights, one reflected off the retina and the other off a reference mirror. The light reflected from the retina includes

contributions from light reflected from the proximal and distal boundaries of the RNFL. An algorithm in the commercial software estimates these boundaries, and the RNFL thickness.

Figure 3A shows a portion of the RNFL thickness report produced by commercial software. Figure 3B shows an enlargement of the results of the scan of the right eye of this individual with normal vision. The circular scan path, made on the peripapillary retina just surrounding the optic nerve, starts in the temporal retina (at 9 o'clock for the right eye) as shown in Fig. 3C. The RNFL thickness is derived with an algorithm that determines the boundaries of the RNFL as shown by the white lines in Fig. 3B. The distance between these white lines is the RNFL thickness and is shown as the black curve in the upper panel of Fig. 3A. This panel is expanded in Fig. 3D. The black curve shows the thickness of the RNFL around the disc going from the temporal position (9 o'clock for the right eye) plotted at position 0 to the nasal position (3 o'clock for the right eye) plotted at position 127 and back to the temporal position plotted at position 255. (Note that the 256-point scale was multiplied by 360/256 to convert it to degrees in the figures below.) The green, yellow and red portions of these graphs are the 95% (upper border of the green region), 5% (yellow) and 1% (red) limits for age-matched normal controls.

The black curve in Fig. 3D, which we will call the "RNFL thickness profile" or "RNFL profile", has two peaks, one in the superior and one in the inferior region of the disc region. These peaks are thought to correspond to the arcuate regions (Figs. 3E,F), although they are also influenced by the presence of blood vessels (see Hood et al. (2007c) and Section 8.2). Notice that the temporal disc receiving input from the papillomacular bundle (orange in Fig. 3E,F) and the nasal disc (purple in Fig. 3E,F) receiving input from the peripheral retina have the thinnest portions of the normal RNFL profile.

3. Mapping of visual field regions to optic disc sectors

3.1 Background

The RNFL report includes a number of summary measures of the RNFL profile (black curve) including the overall average RNFL thickness, as well as the thickness of the sectors of the RNFL profile divided into 4 quadrants and 12 clock hours (e.g. see circles in Fig. 3A). However, these arbitrary divisions do not serve our purpose here. We are interested in the quantitative relationship between the thickness of the RNFL, on the one hand, and the decrease in function in the corresponding area of the visual field measured with the 24-2 SAP field on the other. Therefore, it is important that this comparison is made using portions of the RNFL profile that correspond to regions of the 24-2 SAP field.

3.2 The Garway-Heath et al. map of field location to optic disc location: a working model

A number of studies have produced a map relating regions of the visual field to sectors of the optic disc (e.g. Wirtschafter et al., 1982; Yamagishi et al., 1997; Anton et al., 1998; Weber et al., 1990; Garway-Heath et al., 2000, Garway-Heath et al., 2002, Gardner et al., 2005). The most complete of these maps, from Garway-Heath et al. (2000), is shown in Fig. 4A. In their map, the optic disc is divided into 6 sectors (left panel). Three regions of the visual field (right panel) corresponding to the nasal half of the disc, shown as light gray and white areas, fall mainly outside the boundaries of the 24-2 SAP field. However, the 3 temporal disc sectors, shown in red, blue and dark gray, fall completely within the 24-2 SAP field. In particular, the central macular region (dark gray) of the SAP field is associated with the temporal sector of the disc from 311 to 40 degrees; the superior arcuate region of the visual field (red) is associated with the inferior temporal (red) sector from 271 to 310 degrees; and the inferior arcuate region of the visual field (blue) is associated with the superior temporal (blue) sector from 41 to 80 degrees. The vertical blue and red lines in Fig. 4B show the disc sectors corresponding to the superior and inferior arcuate regions of the field. An axis indicating the distance around the

disc in degrees has been added to the top of this figure. [Note that the map in Fig. 4A differs from the more recently published map by Garway-Heath et al. (2002). For the later, the disc was divided into sectors to match the divisions of the software of the Heidelberg Retina Tomograph (Heidelberg Engineering, Heidelberg, Germany), an instrument that was not used in our studies.]

Figure 4C shows the average RNFL thickness for the right eyes of 50 healthy controls plotted against distance in degrees. On average, the peaks in the superior and inferior nasal sectors of the disc fall within these regions (the boundaries of the superior and inferior arcuate sectors are defined by the parallel red and blue lines), although interestingly they do not fall in the center of these sectors.

3.3 Measuring RNFL thickness and SAP sensitivity loss

Our approach is to compare the SAP field sensitivity in the arcuate visual field regions to the RNFL thickness of the corresponding sectors of the disc. To illustrate this approach, consider the SAP fields and OCT RNFL profiles of a patient with asymmetrical glaucomatous damage (Fig. 5). The SAP report for this patient was shown in Fig. 2; the total deviation values and probability plots of both eyes are displayed in Fig. 5A. As seen in Fig. 5A, there is a clear arcuate defect in the superior visual field of the right eye. The region of decreased sensitivity includes the superior arcuate region, enclosed in red, of the Garway-Health et al. map (Fig. 4). The lower field of the right eye, and the entire field of the left eye, appears normal on the SAP test. The OCT RNFL profiles of the two eyes (Fig. 5B) show good qualitative agreement with the 24-2 SAP results. Notice that the profiles of the two eyes, superimposed in the lower panel in Fig. 5B are approximately the same, except for the inferior section of the disc. For portions of the inferior sector of the disc, the RNFL profile of the right eye (solid curve in bottom panel of Fig. 5B) falls well below that of the left eye (dashed curve). The thinned region includes the RNFL sector between the red lines associated with the inferior arcuate field region.

To make a quantitative comparison between the RNFL thickness and loss of sensitivity in these arcuate regions, we need a quantitative measure of both the RNFL thickness and the SAP sensitivity loss. For the former, the points within the boundaries of the red and blue vertical lines in Fig. 5B are averaged. In this example, the RNFL thicknesses for the inferior temporal disc region (between the red vertical lines) were 156.5 μm (OS) and 47.5 μm (OD). This supplies the estimates of the superior and inferior temporal RNFL thickness for this scan of this patient.

To obtain a measure of the loss in sensitivity for the corresponding arcuate regions of the SAP field, the total deviation values within each of the regions enclosed by the red and blue regions in Fig. 5A were combined. In particular, the anti-log of each value was obtained and these anti-logged values averaged. This average value is our measure of relative sensitivity, with a value of 1.0 indicating that sensitivity was identical to the sensitivity of age-matched controls and a value of 0 indicating that there was no sensitivity to light. To plot SAP field loss in dB units, these averaged values were logged and converted back to a dB scale. For example, 1.0 on a linear scale corresponds to 0 dB (no loss in sensitivity) and a value of 0.001 on a linear scale corresponds to a loss of −30 dB. In Fig. 5A, the relative sensitivity for the upper arcuate region (enclosed in red) was 0.07 or −11.7 dB. Note that had we averaged the dB values for this region without first taking the antilog, the value would have been −24.7 dB.

We have previously explained why it is important to take the anti-log before averaging the measures of the SAP (Hood and Zhang, 2000; Hood and Greenstein, 2003). For the interested reader, the argument will be briefly summarized here. Consider the example in Fig. 6. Suppose an arcuate region had two portions, one with a normal complement of RGCs and the other with all the RGC destroyed. Suppose further that the SAP total deviation was 0 dB (normal

sensitivity) in the region with the normal RGCs and −30 dB (essentially the maximum loss in sensitivity that is measurable) in the region without RGC. The average of the total deviation values is −15 dB, about 1/30 on a linear scale, while the average after first taking the anti-log is 1/2 the normal value or about −3 dB. It seems likely that the RNFL thickness will be closer to 1/2, rather than 1/30, of the normal value. In any case, the linear model to be described below makes this assumption and thus averaging the anti-logged values is the correct way to test the model.

4. Structure versus function: data and a simple linear model

4.1 The data

Figure 7B shows data from three of our recent studies comparing RNFL thickness to SAP field loss for the upper (left panel) and lower (right panel) arcuate regions as defined in Fig. 4A and Fig. 7A. For example, the arrow in the left panel is the point for the superior SAP field region/ inferior disc sector for a single eye plotted at (43.0 μm, −15.4 dB), that is, this glaucoma patient had a RNFL thickness of 43.0 μm in the inferior temporal disc sector and a loss in sensitivity of −15.4 dB in the upper arcuate field region. The filled black circles show the results for 15 eyes with glaucoma (Hood et al., 2007a), the filled gray symbols the results for 24 patients with anterior ischemic optic neuropathy (AION) (Hood et al., 2007b) and the open circles the results for 16 patients with severe glaucoma with MD values worse than −10 dB (Hood et al., 2007c). The larger open square is the mean of a group of 60 controls between the ages of 50 and 79. The 60 controls are all over 50 yrs of age and come from a larger group of individuals studied by Kardon et al., 2007. Their average age (59.6 yrs) was similar to that of the patients with glaucoma and AION (average age of 60.7 yrs). The associated vertical line shows the limits (± 2 SD) for this group.

In Fig. 7B, the results for the patients with AION (gray filled circles) follow a similar pattern to the eyes with glaucoma (black open and filled circles). For arcuate regions with near normal sensitivity (near 0 dB loss), the values of the RNFL thickness in Fig. 7B fall within the normal limits (black vertical lines). On the other hand, for losses in sensitivity greater than about −10 dB, the values approach an asymptotic limit around 45 μm. (The outlier indicated by the asterisk will be discussed in Section 8.1). The smooth curves are predictions from a model to be described below.

At least 5 published studies show plots of OCT RNFL thickness versus SAP sensitivity (Zangwill et al., 2000; El Beltagi et al., 2003; Karnamori et al., 2003; Leung et al., 2004; Sihota et al., 2006). The analysis in these studies is not optimal for testing our model as dB values were averaged and, in general, larger regions of the field compared. However, these studies are in agreement with our data showing a decrease in RNFL thickness from normal values to asymptotic losses as sensitivity loss decreases from 0 dB to −10 dB or more (see review by Hood, 2007).

4.2 The simple linear model

The shape of the curves relating RNFL thickness to SAP sensitivity loss (Fig. 7B) resembles the results from a comparison of the amplitude of local (multifocal) visual evoked potentials (mfVEP) to local losses in field sensitivity (Hood et al., 2002). Figure 8 shows the average mfVEP amplitude versus SAP field loss for 20 patients, 10 with asymmetrical (i.e. one eye had a normal SAP field) AION and 10 with asymmetrical glaucoma. The smooth curve is a fit of a simple linear model. Hood (2007) suggested that the same general model might describe the RNFL thickness data. Here we briefly describe this model, a version of which can be found in Hood (2007) and Hood et al. (2007a).

The model has three, rather simple, assumptions. In particular, we assume

1. The RNFL thickness, R, measured with the OCT technique, is made up of two components. One component, s (for signal), is the thickness due to the RGC axons. The other component, the residual or base level b, is everything else. That is,

$$R = s + b. \tag{1}$$

The residual b undoubtedly includes glial cells and blood vessels and will be affected by the algorithm determining RNFL thickness as well (see Section 8.2).

To get a better estimate of the asymptotic loss in RNFL thickness, the residual b, patients with severe glaucoma and AION were studied. [See gray filled circles (AION) and open black circles (severe glaucoma) in Fig. 7B.]

2. As SAP field sensitivity decreases, the value of s, the thickness due to the axons, decreases, but the residual level b, which is the asymptote, does not change.

3. The relationship between the loss in axons thickness, s, is linearly related to the loss in sensitivity on a linear, not dB, scale. For example, if a region of the field has a total deviation of −3 dB, then the thickness s of the RGC axons for that region will be only 1/2 (anti-log of −3 dB) its initial value. Similarly, if the total deviation is −10 dB, then s will be 1/10 its initial value.

Formally, the RNFL thickness, R, measured with OCT is:

$$R = s_o T + b \quad \text{for } T \leq 1.0 \tag{2a}$$

$$R = s_o + b \quad \text{for } T \geq 1.0 \tag{2b}$$

Pwhere T is relative sensitivity and is equal to $10^{0.1 \times D}$ where D is the total deviation value in dB from the mean age-matched normal value; s_o is the value of s in eq. 1 when sensitivity is normal (T=1.0); and b is the residual thickness. Notice that according to eq. 2b, the RNFL thickness R does not increase if the sensitivity is greater than normal. That is, we are assuming that SAP sensitivity is independent of RNFL thickness in the healthy eye where T≥1.0. Figure 9A shows the predictions of the model (i.e. eqs. 2a and 2b) plotted on linear coordinates.

For the log-linear plot as in Fig. 9B, RNFL thickness, R, is plotted against D, the mean total deviation on a log scale. As $T = 10^{0.1 \times D}$, eq. 1 becomes

$$R = s_o 10^{0.1xD} + b \quad \text{for } D \leq 0 \tag{3a}$$

$$R = s_o + b \quad \text{for } D \geq 0 \tag{3b}$$

Figure 9B shows the predictions of the model (i.e. eqs. 3a and 3b) plotted on semi-log coordinates.

4.3 Fitting the model to the data

In Figs. 7B and 9B, the predicted curve starts at $R = s_o + b$, when D ≥ 0 dB (no loss in sensitivity), and asymptotes at R = b, for large losses in sensitivity (e.g. D = −30 dB). To determine the predicted curves in Figs. 7B, the value for the age-matched normal controls (open square) was taken as the estimate of $(s_o + b)$, the thickness when sensitivity is normal. The value of b was estimated as 33% of the value of the starting point $(s_o + b)$. The rationale for taking 33% as the estimate of b will be described below (Section 5.2). (See the figure caption for the values

of $[(s_o + b), b]$). It is important to note that the data from the patients are not used in generating the theoretical curve. Once the mean value in RNFL thickness of the control eyes with normal sensitivity is determined, the theoretical curve is generated.

The predicted (solid) curve does a good job of describing the data in Fig. 7B. In fact, as we will see below the model actually predicts that the points should fall within the envelope bounded by the dashed lines.

5. The residual RNFL thickness

5.1 The residual RNFL thickness under conditions of severe field loss

According to the model, there is some minimum value beyond which the measure of RNFL thickness cannot be reduced. This assumption needs to be better specified as it leaves unanswered several key questions such as: What is the value of b for the arcuate regions? Does the value of b vary among individuals? Does it vary with location around the disc? Because glaucomatous damage progresses slowly, glaucoma is not the ideal disease for answering these questions. At any given moment in time, it is not clear how many RGC axons are functioning abnormally, but not yet atrophic. AION, on the other hand, has the advantage of being a static optic neuropathy, if measured after the acute stage when atrophy of RGCs has taken place. For this reason, we studied 24 patients who had their last attack of AION at least 5 months prior to our study (Hood et al., 2007b).

The data from the AION patients in Fig. 7B (gray symbols) provide an estimate of the residual RNFL thickness b. In particular, we assumed that the RNFL thickness for SAP losses greater than −10 dB provides an estimate of b. (The theoretical curve approaches its asymptotic value around −10 dB.) There were 15 patients (21 hemifields) in which the arcuate regions had losses greater than −10 dB. We combined the data from the upper and lower arcuates to get 15 estimates, one for each of the 15 patients. The median value, 45.5 μm, provides an estimate of the residual RNFL thickness, b, for the arcuate regions. This value is reasonably close to the value of 44.9 ± μm reported by Sihota et al. (2006) for the average overall RNFL thickness in patients who have lost light perception due to glaucoma. It is also close to the median (mean) value, 43.4 (45.4) μm we obtained from 16 patients with severe glaucoma.

5.2 Variations among individuals in the residual thickness: a working hypothesis

The residual (asymptotic) thickness b shows considerable variation among individuals as evidenced by the scatter around the asymptote of the theoretical curve in Fig. 7B. While there are various possible reasons for the variation in this residual thickness, we suggested that part of the variation represents a difference among normal individuals in the non-axonal content of the RNFL (Hood et al., 2007b). The data from the AION patients provide a means for estimating the extent of the non-axonal contribution, b, to the RNFL thickness.

The RNFL thickness profiles for the two eyes of a normal individual are very similar (see Figure 3A and Ghadiali et al, 2007). Thus, we can use the RNFL thickness of the unaffected eye of AION patients as an estimate of the RNFL thickness of the affected eye before vision became impaired. The residual b values for 9 patients with unilateral AION are plotted against the thickness of the corresponding region of the fellow (unaffected) eye as the filled circles in Fig. 10. The solid line shows that there was a good linear correlation (r=0.94) between the residual RNFL thickness, b, in the affected eye and the RNFL thickness, $s_o + b$, in the unaffected eye. To a first approximation, the residual thickness is about 1/3 (33%) of the initial/healthy thickness as indicated by the dashed line with a slope of 1/3. [As will be discussed below (Section 7.4), the relationship is different for the central visual field/temporal disc as indicated by the open symbols in Fig. 10.]

As a working hypothesis, we assume that the residual RNFL thickness in the arcuate regions varies among individuals and is approximately 33% of the RNFL thickness when this region is healthy (i.e. has no sensitivity loss). Further, this provides a procedure for estimating the average value of the residual RNFL (b) for the theoretical curves in Fig. 7B. As mentioned above, the value of b was taken as 33% of the RNFL thickness for 0 dB loss in sensitivity (normal RNFL thickness). This produced estimates of b for the upper (42.4 μm) and lower (47.5 μm) fields that were close to median asymptotic value, 45.5 μm, estimated from the combined data from the upper and lower fields.

5.3 The range of predictions for the linear model

The dashed curves in Figs. 7B show the ± 2SD limits for the predictions of the model. They were derived in the following way. First, we assume that the 95% limit of the RNFL thickness of normal individuals is approximated by the vertical lines in Figs. 7B. Recall that these are the ± 2 SD limits of a group of normal individuals of similar age. The ±2SD limits for the lower arcuate RNFL thickness range from 109.8 to 178.0 μm. Second, we assume that the residual thickness is 33% of these values or 36.6 and 58.7μm, respectively. Thus, the upper dashed curve in Fig. 7B (left panel) goes from 178.0 to 58.7 μm and the lower dashed curve from 109.8 to 36.6 μm. The dashed curves in Fig. 7B (right panel) were derived in a similar way. These dashed lines provide an envelope of predicted curves for different individuals depending upon their initial RNFL thickness. Points may, of course, fall outside these limits due to measurement error and other sources of variability.

While the linear model does a good job of describing the patients' data in Fig. 7B, there is a key assumption that needs to be addressed. In particular, the model assumes that RNFL thickness does not change if sensitivity is greater than normal. We consider a test of this assumption next.

6. RNFL thickness and field sensitivity in healthy individuals

To test the relationship between visual field sensitivity and RNFL thickness in healthy individuals, the results from 82 controls were examined (Kardon et al, 2007). The open symbols in Fig. 11 show the results for the 60 of these controls older than 50 years of age, a group with an age distribution similar to the patients. The filled symbols show the results grouped into bins of 10 individuals after ranking them by field loss. According to the model (eq. 2b), the RNFL thickness for the healthy controls should not vary with visual field sensitivity and thus should fall along a horizontal line. There is a weak positive correlation for both the upper (r=0.29; slope=4.0 μm/dB) and lower (r=0.22; slope=4.1 μm/dB) arcuate field regions. Perhaps, there is a small increase in sensitivity associated with a larger number of RGCs and a thicker RNFL. In any case, the grouped data (filled symbols) fall close to model's prediction (the middle dashed line). To put the small deviation from our model into perspective, consider an alternative model that assumes that the relationship between RNFL thickness and sensitivity is the same for both controls and patients. (That is, assume that eqs. 2a and 3b hold for all values of T or D.) This version of the model would predict that the data in Fig. 11 should fall along the gray curve.

While our model (eq. 3b) predicts the general form of the control data in Fig. 11, it is does not address the wide range of RNFL thickness among healthy individuals. Note, for example, that the RNFL thickness ranges from 114.6 to 182.2 μm in Figs. 11A and from 83.4 to 166.1 μm in Fig. 11B. There are a number of factors that contribute to this range of values in healthy eyes; some of these are discussed in Section 8.

7. Structure versus function in glaucoma revisited

It is commonly held that structural damage precedes functional damage in glaucoma. However, this statement can mean different things to different people. Here we consider our model in light of three possible meanings of this statement, a fourth possible meaning will be discussed in section 9.1.

7.1 Which test will detect early glaucomatous damage first?

According to the linear model, functional damage (loss in SAP field sensitivity) is related linearly to structural damage (loss of RNFL thickness due to axons). Thus, if the linear model is correct, then structure does not precede function, nor does function precede structure. *The strict answer according to the model is that they occur together.* In other words, RNFL thickness is linearly related to SAP loss. However, if the question is which test will show *statistically significant* glaucomatous damage first, then the answer depends upon the relative variation in the test measurements of structure and function among normal eyes. A test with a larger standard deviation among normal eyes, all else being equal, would require a larger deficit to reach statistical significance than would a test with a smaller standard deviation.

Figure 12 illustrates this point using our theoretical curves for the superior arcuate field/inferior temporal disc from Fig. 7B (left panel). In Fig. 12, OCT thickness for the inferior disc sector is compared to the loss in sensitivity in the upper arcuate region of the SAP field. The dashed, horizontal, dark gray line indicates the lower 2.5% limit for the RNFL thickness of a control group, while the vertical, light gray vertical dashed line is the lower 2.5% limit for the SAP field test of a control group. That is, 97.5% of the normal RNFL thickness values fall above the horizontal dark gray line and 97.5% of the normal SAP values fall to the right of the vertical light gray line. It is important to note that points falling in the upper right quadrant defined by the intersection of the vertical and horizontal lines represent test results for which both tests were normal, while those falling in the lower left represent test results for which both test results are abnormal. The interesting quadrants are those in which one test is normal and the other is abnormal. In particular, test results in the upper left quadrant signify a normal RNFL thickness, but an abnormal SAP result. On the other hand, a test result in the lower right quadrant signifies a normal SAP test, but an abnormal RNFL thickness.

According to the model, if we ignore measurement error, 95% of the points should fall between the black dashed curves in Fig. 12. The shaded regions indicate the location of points for which the RNFL and SAP tests disagree. In particular, a point that falls in the smaller light gray region has a statistically abnormal SAP test, but a normal RNFL thickness. On the other hand, a point that falls in the larger dark gray region has a statistically abnormal RNFL thickness, but a normal SAP test. *Thus, for the upper arcuate field, the model predicts that for the patients for whom the two tests disagree, more will show significant RNFL loss and normal SAP results than will show significant SAP loss and a normal RNFL thickness.* Notice that changing the confidence limits of either test will change the relative sizes of the regions in gray and hence the proportion of patients with statistically significant structural loss preceding functional loss. For example, anything that increases the variability of the SAP field results (e.g. inexperienced field takers) would result in a larger dark gray area and a smaller light gray area.

Thus, there is no discrepancy between the model and the statement that structure precedes function, if by "structure precedes function" one means that a structural test can show *statistical significance* before a functional test does. [For related arguments see Hood et al., 2002, Hood and Greenstein, 2003; Garway-Heath, 2004; Harwerth et al., 2007.]

7.2 Does a loss of RGC axons really precede visual field loss?

By 'structural damage precedes functional damage' some people mean that *substantial RGC loss precedes a loss in SAP sensitivity*. Further, this statement has at least two meanings. On the one hand, a "statistical RGC interpretation" of this statement could mean that a statistically significant RGC loss occurs before a statistically significant SAP loss can be detected (as discussed in the prior section). This interpretation is not in conflict with our model. In fact, for the conditions of Fig. 12, a linear model predicts that the lower boundary of the SAP confidence limit (i.e. −2.4 dB or a 42% loss in sensitivity) is associated with approximately a 42% RGC loss (see eq. 3A).

On the other hand, a "relational RGC interpretation" of 'RGC loss precedes a loss in SAP sensitivity' could mean that the mathematical relationship between SAP loss and RGC loss is not monotonic. In particular, some people believe that no sensitivity loss of SAP loss occurs until 25 percent or more of the RGCs are lost. This interpretation would be in conflict with our model. However, the published data do not provide strong support for either the statistical or relational interpretation of "RGC loss precedes loss in SAP sensitivity". A complete review of this issue is beyond the scope of this article, but a consideration of a few of the most commonly referenced papers is warranted.

Kerrigan-Baumrind et al. (2000) compared SAP field loss to post-mortem RGC counts in humans. They concluded that a statistically significant SAP field defect did not occur until 25% to 35% of the RGC's were lost. To calculate the RGC loss, they compared the RGC counts postmortem in glaucoma patients to those in a group of normal controls. However, a 25–35% loss in RGC count relative to the mean RGC count in normal eyes is *not* statistically significant as it fell within the 95% confidence limits of their normal RGC counts. Thus, the 'statistical interpretation' of the statement that 'RGC loss precedes loss in SAP sensitivity' is not supported. Further, when they plotted local SAP sensitivity loss against local RGC loss for 429 pairs of local field points, the correlation (r^2) was only 0.03. That is, there was no support for an association between the functional test result and RGC loss under their measurement conditions and in their group of glaucoma patients. In other words, there was also no support for the 'relational RGC interpretation' of the statement that 'RGC loss precedes loss in SAP sensitivity'. In fact, according to the regression line fitted to their scatter plot of MD (mean deviation) versus percent of normal RGC, 100% of normal RGC count was associated with a MD worse than −6 dB, i.e. a significant field loss (see their Fig. 3). In other words, a normal RGC count was associated with a −6 dB loss, i.e. SAP sensitivity loss *preceded* a loss of RGCs (Garway-Heath, 2004). While RGC loss may precede the detection of SAP field loss in humans, the data from Kerrigan-Baumrind et al. (2000) do not provide strong support for this contention.

In an elegant series of papers, Harwerth and colleagues (e.g. Harwerth et al., 1999; Harwerth et al., 2002) compared post-mortem RGC counts to behavioral SAP sensitivity loss in monkeys with experimental glaucoma. Unlike the human work, they could measure RGC loss more accurately relative to the normal state because the non-glaucomatous opposite eye served as the control and the RGC counts from the two eyes of a normal monkey are similar. While their work is often taken as support for the Kerrigan-Baumrind et al. conclusion, their monkeys showed, on average, a functional loss greater than −6 dB even when the average RGC loss was minimal, less than 10% (see Fig. 2B in Harwerth et al., 2002). That is, a significant SAP field loss, on average, was associated with minimal RGC loss. Thus, while there may be significant RGC loss before SAP tests are abnormal, the current primate data on post-mortem counts provide weak support for this idea.

7.3 Relationship to other models

Recently, Harwerth et al., 2007 proposed a model that relates OCT RNFL thickness to SAP sensitivity loss in monkeys. While their model is framed in a very different form, it can be reformulated in a form similar to our model (Section 4.2). In particular, they found that log RGC count is linear with log SAP sensitivity (linear on log axes) (Harwerth et al., 2004). We assume the relationship is linear on linear axes. [If the slope of their function were 1.0, then we would be in agreement. However, their slope ranges from 1.25 to 2.32 depending upon eccentricity in the retina (Harwerth et al., 2004).] Second, they assume that all the RNFL thickness measured with the OCT is attributable to RGC axons. Thus, there is no residual thickness in their model. As shown above, there is a residual RNFL thickness, b, which remains after all sensitivity to light has been lost (Fig. 7B). Third, they found that in the normal eye, the SAP sensitivity varies with RGC count and, thus, RNFL thickness. In contrast, we have shown that, to a first approximation, the sensitivity of normal eyes does not depend upon RNFL thickness (Fig. 11).

The black curves in Figure 13 show the fit of a model, based upon their assumptions, to our data from Fig. 7B with our model's predictions shown as the gray curves. To be fair, we did not fit the model in the same way that they did. To fit the model, we made the assumptions directly above plus we assumed that the slope of the function relating RGC axons to SAP loss was 1.5, the value they give for an eccentricity of 10°. If we allow for the same residual as in our model, then a model based upon their assumptions yields the dashed black curve. (In fact, the current, unpublished version of their model has a residual portion assumed to consist of glial cells (R. Harwerth, personal communication.) This dashed curve is close to the mean prediction of our model (gray curve), although it does not fit our data quite as well. Further work is needed to see if the data from controls and patients can distinguish between our model and theirs.

Garway-Heath and colleagues have argued that structural measures (e.g. neural rim) more closely approximate a linear function if plotted against linear SAP loss, as opposed to log SAP loss (Garway-Heath et al., 1999; Garway-Heath et al., 2002; Garway-Heath, 2004). While their work is consistent with a linear model, it does not specify the precise linear relationship (i.e. the slope and intercept of the linear function) between structural loss and SAP field loss. It would be of interest to see if their structural and electrophysiological data can distinguish between the linear model described here and other plausible alternatives.

Swanson et al. (2004), building upon aspects of previous models of spatial vision, proposed a theoretical framework for predicting the loss in SAP sensitivity with local loss in RGC. The details of their psychophysical model are relatively complicated, but the essence of the predictions can be explained fairly simply. For peripheral visual field sensitivity, the SAP threshold (expressed in linear not dB units) will decrease linearly with percent RGC loss. They concluded that, for these conditions, their model supported the Hood et al. (2002) prediction of a linear relationship between behavioral loss in sensitivity and RGC loss. However, for central visual field sensitivity at the fovea, SAP sensitivity loss is predicted to decrease less rapidly with RGC loss than the loss predicted by our linear model. In the next section, we examine the data for the central portion of the SAP field.

7.4 The papillomacular bundle and the linear model

Our initial tests of the linear model were restricted to the arcuate regions as defined in Fig. 4. We chose to focus on these regions because they were completely within the 24-2 SAP field and they are the sites of early glaucomatous damage. The question naturally arises as to whether the data for the central macular field region and the associated papillomacular bundle (dark gray in Fig. 4A) also can be described by the linear model. Because of the greater density of

RGCs in the macula, a different model may describe the results (for example, see Swanson et al., 2004 in Section 7.3).

Figure 14A shows the central field results for the 24 patients with AION (gray circles), the 15 patients with asymmetrical glaucoma (black circles), and the 16 patients with severe glaucoma (open circles). Here the RNFL thickness of the papillomacular sector (dark gray in Fig. 4A-left panel) is plotted against the field loss in the central macular region (dark gray in Fig. 4A-right panel). As in Fig. 7B, the vertical line at 0 dB is the 95% confidence limit for RNFL thickness for the same age-matched control group. The curves are the predictions from the model. These curves have their starting points at 0 dB based upon the mean of the controls (solid curve) and the end points of the confidence interval (dashed curves). The formula for estimating the asymptote, b, of these curves was taken, as in the case of Fig. 7, from the AION data for the asymmetrical patients. In the case of the papillomacular sector, the residual thickness is no longer simply 33% of the normative value (see equation in figure caption). As can be seen in Fig. 10, the relationship between the residual b and the RFNL thickness in the healthy eye for the papillomacular bundle (open squares) was different from that of the arcuate regions (filled symbols). In particular, the residual thickness for the macular region tended to be a relatively larger percentage of the total RNFL thickness than the 33% value found for the arcuate regions, suggesting a larger proportional contributions from non-axonal elements (e.g. glia and blood vessels) to the RNFL thickness of the papillomacular bundle.

Figure 14B shows the central data for the 60 controls plotted as in Fig. 11. As in the case of the arcuate regions, there is a weak positive correlation (solid black line: r=0.17; slope=1.9 µm/dB). However, the grouped data (filled symbols) fall far from the predictions (gray curve) of a model that assumes that the same relationship (eq. 3a) between RNFL thickness and sensitivity holds for both controls and patients. The OCT thickness for the central region is relatively independent of the sensitivity in this region for healthy eye. The model (eq. 3b) describes the central data in Figs. 14A,B reasonably well. The points in Fig. 14A fall, in general, between and around the dashed curves and, the best fitting line (solid) for the control data in Fig. 14B is close to the line (middle dashed) predicted by the model (eq. 3b).

According to the Swanson et al (2004) model, more points should fall below the solid theoretical curve in Fig. 14A, than fall below the solid curve in Fig. 7, at least for the early part (up to −10 dB or so) of the curve. However, the difference between the Swanson et al predictions and those of our model are subtle compared to the spread in the RNFL thickness values. Other methods are needed to distinguish between these predictions.

8. Improving the model

The model predicts that 95% of the points for individual patients should fall between the dashed curves in Fig. 7B. It is clear from this figure that there are some points that fall above or below the theoretical predictions. In principle, as the SAP sensitivities are corrected for age, we should correct the OCT values as well. However, in practice, the effect of age on OCT thickness is relatively small and age accounts for very little of the variance in the data (e.g. Bowd et al., 2000;Hougaard et al., 2006;Budenz et al, 2007;Parikh et al, 2007). On the other hand, some of the variation from the model in Fig. 7B is due to measurement error in either the SAP sensitivity or RNFL thickness. For example, eye position relative to the scanning circle affects the RNFL profile and the RNFL thickness measurement within the arcuate regions. The black curves in Figure 15 show the effects on the RNFL profile when the position of the disc relative to the circular scan location is changed in the vertical or horizontal position. The profiles change in predictable and systematic ways (see figure caption). For the data reported in this review, care was exercised to minimize measurement error by careful alignment of the scan and by using OCT scans with high signal to noise ratios. In any case, measurement error is unlikely to

account for the entire scatter and outlier points in the data. Here we identify two other factors that are undoubtedly involved.

8.1. Variation in mapping of field region to disc sector

The ability of any model relating structure to function to predict the actual data depends on a map that accurately relates specific SAP field regions to their corresponding RNFL sectors. The Garway-Heath et al. (2000) scheme in Fig. 4 represent one map based upon data from many individuals. Individuals may deviate from this average map, although relatively little is known about this deviation. Garway-Heath et al. note that the uncertainty of these measurements was on the order of 30° (95% confidence interval). A patient who deviates from this average map may appear as an outlier on plots such as Fig. 7B.

In fact, we have argued that the outlier in Fig. 7B (asterisk in left panel) is an example of patient whose map deviates from the scheme of Garway-Heath et al (Hood et al, 2007a). Figure 16A is a reproduction of Fig. 7B (left panel). The outlier (filled circle with the downward arrow) is not the result of measurement error as indicated by the measures repeated on different days and shown as the + symbols. These repeat measures have similar RNFL thicknesses and all fall well outside the boundaries defined by the theoretical lines. The arrow and the filled red symbol in Fig. 16A show the RNFL thickness that would bring the point in line with the mean theoretical curve. The dashed lines in Fig. 16B show the shift in the location of the disc sector required to yield a thickness predicted by the mean line. If this patient's map of superior field to inferior arcuate sector was 21.1° more nasal than the Garway-Heath et al map predicts, then the point would now fall on the mean theoretical line. Note it would have to be off by even less to fall on the upper dashed curve. The most likely explanation for this outlier is that the map relating field region to disc sector deviates from the norm in this eye and indicates how a different mapping can be the cause of an outlier in plots such as Fig. 7B.

8.2. The influence of blood vessels

The contribution of blood vessels (BVs) to RNFL thickness measurements represents another possible source of deviation from the linear model. BVs can influence the RNFL thickness measured with OCT. The arteries coming from, and the veins going to, the optic disc are found in the RNFL and contribute to its thickness. Although the presence of these BVs can be inferred from the shadows they cast (Fujimoto et al., 2004), little has been written about how they influence the RNFL profile. To obtain an estimate of the contribution of the BVs to the RNFL thickness, Hood et al. (2007c) examined the relationship between the location of the BVs and the local maxima in the RNFL profiles of controls and patients with severe field loss due glaucoma. Figure 17 illustrates some of their findings with a patient with AION. Figure 17A shows the disc photo and Fig. 17B the RNFL profile of the unaffected, right eye of a patient who experienced AION in the left eye 12 months prior to this scan. The locations of the four prominent maxima in the RNFL profile of the better eye are indicated in the lower panel of Fig. 17B with the 4 colored lines. These locations were transferred to the fundus photo in Fig. 17A. There is a good correspondence between the locations of the peaks in the RNFL profile (Fig. 17B, lower panel), the shadows in the scan (Fig. 17B, upper panel), and the major BVs in the disc photo (Fig. 17A). The BVs are contributing to the RNFL profile and, in particular, help to determine the local maxima (Hood et al., 2007c). The scan of the affected eye in Fig. 17D provides an estimate of the size of this contribution. Although the patient retained a visual acuity of 20/25, this eye had lost nearly all sensitivity to light as measured with the SAP (Fig. 17C). In particular, the patient was not able to detect the test spot placed within, or just outside, the arcuate regions. The residual RNFL thickness in the corresponding portions of the disc (within the vertical dashed blue and red lines) must be due largely to the BVs. The red arrows on the scan in Fig. 17D indicate local regions of thickening within, and just outside, the arcuate regions (vertical, dashed lines). Note that these thickenings occur in regions showing shadows,

indicating the presence of BVs. A red rectangle encloses one of the supposed BVs in Fig. 17D, which is also shown in the inset. The region within the red rectangle is about 150 μm wide and 150 μm thick, in the range of what one should expect of a major BV (Wise et al., 1971).

The BVs contribute to the RNFL thickness and to the variability in the RNFL profiles among individuals (Hood et al., 2007c). In fact, the location of the major BVs may supply a way to identify inter-individual variations in mapping. In particular, the location of the superior (inferior) peak in the RNFL profile corresponds to the location of the superior (inferior) temporal vein and artery (Hood et al., 2007c). Although the RNFL peaks are shaped in part by the BVs, they are largely shaped by the RGC axons, which, in general, have their greatest density near the inferior and superior temporal retinal veins and arteries. Thus the marked variation in the location of BVs in the temporal region of the disc may be predictive of the variations in structural-functional mapping in the arcuate regions.

However, in some cases the algorithm does not include the entire residual thickness due to the BVs. Notice in Fig. 17D, for example, that the algorithm did not include the entire BV thickness in the upper disc (left two arrows). That is, the signal from these two BVs is thicker than the distance between the white lines set by the algorithm. Because the OCT algorithm involves considerable spatial averaging, local perturbations may be ignored. On the other hand, most of the thickness of the cluster of two BVs in the lower disc region (right two arrows in Fig. 17D) is included between the white lines set by the algorithm in the upper panel of Fig. 17D. In any case, the BVs in both upper and lower arcuate regions (all 4 arrows) are presumably included in the RNFL thickness of the better eye where they contribute to the amplitude and shape of the peaks. With severe damage, the residual RNFL contains a contribution due to the BVs, as well as probably a contribution from glial cells. The size of the BV contribution may decrease in part due to a decrease in the size of the BVs in patients with glaucoma (e.g. Jonas et al, 1991;Rader et al, 1994). However, the shrinkage of the BVs is relative small, about 15% of diameter, according to Jonas et al (1991). The size of the BV contribution to the residual RNFL thickness is more likely to vary based upon whether the algorithm incorporates it into the measurement.

Overall, the BV contribution to the total RNFL thickness is not large, about 13% of the average OCT RNFL thickness (Hood et al., 2007c) and between 0 and 25% in the temporal arcuate sectors depending upon the number of BVs within these sectors. On the other hand, BVs can make a substantial contribution to the residual thickness. In any case, estimating the BVs contribution to individual scans and accounting for this contribution should improve the usefulness of the model, as well as decrease the variability among controls.

9. Summary and future directions

9.1 Implications for the structure versus function debate

It is commonly held that structural damage precedes functional loss in glaucoma. We have argued above that this statement has at least two general meanings. It can refer to a *statistical statement* about whether a structural measure will reach significance before a functional test will. Or, it can refer to a *relational statement* about the mathematical relationship between a structural measure and a functional test. However, we also argued above that by 'a structural measure' some individuals mean actual RGC counts, while others refer to structural tests, such as OCT RNFL thickness or disc appearance. Therefore, there are actually four different questions one could have in mind when asking, 'Does structural damage precede functional damage?' The top portion of Fig. 18 delineates these four meanings. The bottom portion illustrates how the linear model answers each question. For this illustration, assume that by 'function' is meant the SAP test, although other functional tests could be treated in the same framework.

Our model directly contradicts the common answer to the first question, 'Is the relationship between SAP loss and RGC loss non-monotonic?' Some say that substantial RGCs must be lost before SAP sensitivity changes, that is the relationship between SAP loss and RGC loss is not monotonic. Others assume, or at least imply, that the relationship between SAP loss and RGC loss, if not non-monotonic, is at least nonlinear. In particular smaller SAP losses are said to be associated with early RGC loss and with severe disease, larger SAP losses are associated with smaller degrees of RGC loss. Our model assumes that SAP loss, as well as OCT thickness, decreases linearly with RGC axon loss.

The model does not directly speak to the statistical RGC interpretation (question 2). We do not have direct measurements of RGC loss to evaluate whether "statistically significant RGC loss occurs before statistically significant SAP loss". However, we argued that the studies of post-mortem RGC counts in humans and primates have yet to fully answer this question.

On the other hand, the model and the framework in Section 7.1, do propose answers to questions 3 and 4, the questions about structural and functional tests. First, the model explicitly assumes that loss on the SAP functional test is a linear function of RNFL thickness on the OCT structural test. Second, the model predicts that OCT RNFL thickness (a structural test) can show statistical significance before SAP loss (a functional test) in detecting early glaucomatous damage. In particular, the structural test in a patient may be abnormal before the functional test due largely to the fact that the normal confidence limits are greater for the functional test compared to the structural test. In other patients, the functional test may reach statistical significance first. In these cases, the patient started out with more structure to begin with (i.e. they were born with a relatively thick RNFL), so it requires more loss of structure before the RNFL becomes thin enough to drop below the 5th percentile for normal eyes.

In summary, if we are to make progress in understanding the relationship between structural and functional damage in glaucoma, it is essential that we are clear about what is meant by the question, 'How is structural damage related to functional damage?' Does it refer to a statistical finding or a mathematical relationship? And, what is being measured, the actual number of RGC present or the outcome of a structural test. Admittedly, Figure 18 is not the only framework within which to phrase this problem. However, the particular framework is less important than is the need to be explicit.

9.2 Future directions

The linear model, as well as the general approach presented here, suggests a number of directions for future work. First, the general approach provides a framework for comparing any two tests. That is, the approach can be applied to predicting the relative sensitivity of any two tests (e.g. SAP vs Frequency Doubling Perimetry; SAP vs. mfVEP) (Hood and Greenstein, 2003; Hood et al., 2004). To compare two tests, one needs to specify the mathematical function relating the results on one test to the results on the other. If the confidence limits are specified for each of the tests, the relative sensitivity of the two tests can be predicted. Second, it will be interesting to compare the results from patients with loss of vision due to conditions other than glaucoma. The degree to which the model predicts the results from these patients offers both a test of the model and an opportunity to better understand the pathology of the condition involved. For example, a patient with a reversible optic neuropathy (e.g. compressive) would be expected to deviate from the model in a predictable way. In particular, if the loss of vision were due to a temporary dysfunction of the RGCs (e.g. conduction block secondary to compression), then the data point for this patient would tend to fall well above the theoretical curves for the model. Furthermore, such a patient without a clear sign of structural (i.e. RNFL) loss would be expected to have a good prognosis after decompression. In conjunction with other tests, the model could aid in identifying non-organic loss, separating RGC dysfunction from outer retinal pathology, and identifying post-geniculate components of visual loss.

Finally, the model makes a clear prediction about course of progression of glaucomatous damage over time. Any individual patient should follow a single theoretical curve as glaucoma progresses. In general, longitudinal data on the same individuals provide an important testing ground for the model. In particular, an interesting test of the model is to see if a patient's points do indeed fall along a curve as predicted. If so, the model may be of use to the glaucoma specialist facing the clinical challenges of detecting of early glaucomatous damage and/or monitoring its progression over time.

References

Anderson RS. The psychophysics of glaucoma: improving the structure/function relationship. Prog Retin Eye Res 2006;25:79–97. [PubMed: 16081311]

Anderson, DR.; Patella, VM. Automated Static Perimetry. 2. Mosby-Year Book Inc; St Louis: 1999.

Anton A, Yamagishi N, Zangwill L. Mapping structural to functional damage in glaucoma with standard automated perimetry and confocal scanning laser ophthalmoscopy. Am J Ophthalmol 1998;125:436–446. [PubMed: 9559728]

Bowd C, Weinreb RN, Williams JM, Zangwill LM. The retinal nerve fiberlayer thickness in ocular hypertensive, normal, and glaucomatous eyes with optical coherence tomography. Arch Ophthalmol 2000;118:22–26. [PubMed: 10636409]

Budenz DL, Anderson DR, Varma R, Schuman J, Cantor L, Savell J, Greenfield DS, Patella VM, Quigley HA, Tielsch J. Determinations of normal retinal nerve fiber layer thickness measured by stratus OCT. Ophthalmol. 2007In press

Chauhan BC. Detection of glaucoma: the role of new functional and structural tests. Curr Opin Ophthalmol 2004;15:93–95. [PubMed: 15021218]

Costa RA, Skaf M, Melo LA Jr, Calucci D, Cardillo JA, Castro JC, Huang D, Wojtkowski M. Retinal assessment using optical coherence tomography. Prog Retin Eye Res 2006;25:325–353. [PubMed: 16716639]

El Beltagi TA, Bowd C, Boden C. Retinal nerve fiber layer thickness measured with optical coherence tomography is related to visual function in glaucomatous eyes. Ophthalmol 2003;110:2185–2191.

Fujimoto, JG.; Hee, MR.; Huang, D., et al. Principles of optical coherence tomography. In: Schuman, JS.; Puliafito, CA.; Fujimoto, JG., editors. Optical Coherence Tomography of Ocular Diseases. Slack Inc; Thorofare, New Jersey: 2004. 2004

Gardiner SK, Johnson CA, Cioffi GA. Evaluation of the structure-function relationship in glaucoma. Invest Ophthalmol Vis Sci 2005;46:3712–3717. [PubMed: 16186353]

Garway-Heath, DF.; Viswanathan, A.; Westcott, M.; Kamal, D.; Fitzke, FW.; Hitchings, RA. Relationship between perimetric light sensitivity and optic disc neuroretinal rim area. In: Wall, M.; Wild, JM., editors. Perimetry Update 1998/1999. Kugler Publications; The Hague: 1999. p. 381-389.

Garway-Heath DF, Poinoosawmy D, Fitzke FW, Hitchings RA. Mapping the visual field to the optic disc in normal tension glaucoma eyes. Ophthalmology 2000;107:1809–1815. [PubMed: 11013178]

Garway-Heath DF, Holder GE, Fitzke FW, Hitchings RA. Relationship between electrophysiological, psychophysical, and anatomical measurements in glaucoma. Invest Ophthalmol Vis Sci 2002;43:2213–2220. [PubMed: 12091419]

Garway-Heath, DF. Comparison of structural and functional methods. In: Weinreb, RN.; Greve, EL., editors. Glaucoma Diagnosis Structure and Function. Kugler Publications; The Hague: 2004. p. 135-143.2003

Ghadiali Q, Hood DC, Manns CJ, Llinas A, Lin A, Lee C, Greenstein VC, Odel JG, Liebmann JM, Ritch R, et al. An analysis of normal variations in retinal nerve fiber layer thickness profiles measured with optical coherence tomography. 2007Submitted

Girkin CA. Relationship between structure of optic nerve/nerve fiber layer and functional measurements in glaucoma. Curr Opin Ophthalmol 2004;15:96–101. [PubMed: 15021219]

Harwerth RS, Carter-Dawson L, Shen F, Smith EL 3rd, Crawford ML. Ganglion cell losses underlying visual field defects from experimental glaucoma. Invest Ophthalmol Vis Sci 1999;40:2242–2250. [PubMed: 10476789]

Harwerth RS, Crawford ML, Frishman LJ, Viswanathan S, Smith EL 3rd, Carter-Dawson L. Visual field defects and neural losses from experimental glaucoma. Prog Retin Eye Res 2002;21:91–125. [PubMed: 11906813]

Harwerth RS, Carter-Dawson L, Smith EL 3rd, Barnes G, Holt WF, Crawford ML. Neural losses correlated with visual losses in clinical perimetry. Invest Ophthalmol Vis Sci 2004;45:3152–3160. [PubMed: 15326134]

Harwerth RS, Vilupuru AS, Rangaswamy NV, Smith EL 3rd. The relationship between nerve fiber layer and perimetry measurements. Invest Ophthalmol Vis Sci 2007;48:763–773. [PubMed: 17251476]

Heijl, A.; Patella, VM. Essential Perimetry The Field Analyzer Primer. Carl Zeiss □Meditec Inc; Jena, Germany: 2002.

Huang D, Swanson EA, Lin CP, et al. Optical coherence tomography. Science 1991;254:1178–1181. [PubMed: 1957169]

Hood DC. Relating retinal nerve fiber thickness to behavioral sensitivity in patients with glaucoma: The application of a linear model. J Optical Society of America 2007;24:1426–1430.

Hood DC, Greenstein VC. The multifocal VEP and ganglion cell damage: applications and limitations for the study of glaucoma. Progress in Retinal and Eye Res 2003;22:201–251.

Hood DC, Zhang X. Multifocal ERG and VEP responses and visual fields: comparing disease-related changes. Doc Ophthal 2000;100:115–137.

Hood DC, Greenstein VC, Odel JG, Zhang X, Ritch R, Liebmann JM, Hong JE, Chen CS, Thienprasiddhi P. Visual field defects and multifocal visual evoked potentials: Evidence for a linear relationship. Arch Ophthalmol 2002;120:1672–1681. [PubMed: 12470141]

Hood DC, Thienprasiddhi P, Greenstein VC, Winn BJ, Ohri N, Liebmann JM, Ritch R. Detecting early to mild glaucomatous damage; A comparison of the multifocal VEP and automated perimetry. Invest Ophthalmol Vis Sci 2004;45:492–498. [PubMed: 14744890]

Hood DC, Anderson SC, Wall M, Kardon RH. Structure versus function in glaucoma: An application of a linear model. Invest Ophthalmol and Vis Sci. 2007aIn press

Hood DC, Anderson SC, Rouleau J, Wenick AS, Grover LK, Behrens MM, Odel JG, Lee AG, Kardon RH. Retinal nerve fiber structure versus visual field function in patients with ischemic optic neuropathy: A test of a linear model. 2007bIn press

Hood DC, Fortune B, Arthur SN, Xing D, Salant J, Ritch R, Liebmann JM. Blood vessels and axon density contribute to the variation in retinal nerve fiber profiles measured with optical coherence tomography (OCT). 2007csubmitted

Johnson CA. Psychophysical measurement of glaucomatous damage. Surv Ophthalmol 2001;45:S313–8. [PubMed: 11377455]

Jonas JB, Fernandez MC, Naumann GO. Parapapillary atrophy and retinal vessel diameter in nonglaucomatous optic nerve damage. Invest Ophthalmol Vis Sci 1991;32:2942–2947. [PubMed: 1917397]

Hougaard JL, Ostenfeld C, Heijl A, Bengtsson B. Modelling the normal retinal nerve fibre layer thickness as measured by Stratus optical coherence tomography. Graefes Arch Clin Exp Ophthalmol 2006;244:1607–1614. [PubMed: 16788824]

Kanamori A, Nakamira M, Escano MFT, Seya R, Maeda H, Negi A. Evaluation of the glaucomatous damage on retinal nerve fiber layer thickness measured by optical coherence tomography. Am J Ophthalmol 2003;135:513–520. [PubMed: 12654369]

Kardon RH, Hood DC, Anderson SC, Wall M. Measurement variability of structure and function in normal eyes and in glaucoma. 2007In preparation

Kerrigan-Baumrind LA, Quigley HA, Pease ME. Number of ganglion cells in glaucoma eyes compared with threshold visual field tests in the same persons. Invest Ophthalmol Vis Sci 2000;41:741–748. [PubMed: 10711689]

Leung CK, Yung WH, Ng AC, Woo J, Tsang MK, Tse KK. Evaluation of scanning resolution on retinal nerve fiber layer measurement using optical coherence tomography in normal and glaucomatous eyes. J Glaucoma 2004;13:479–485. [PubMed: 15534473]

Parikh RS, Parikh SR, Sekhar GC, Prabakaran S, Babu JG, Thomas R. Normal age-related decay of retinal nerve fiber layer thickness. Ophthalmology 2007;114:921–926. [PubMed: 17467529]

Rader J, Feuer WJ, Anderson DR. Peripapillary vasoconstriction in the glaucomas and the anterior ischemic optic neuropathies. Am J Ophthalmol 1994;117:72–80. [PubMed: 8291596]

Ritch, R.; Shields, MB.; Krupin, T. The Glaucoma. 2. Mosby; St. Louis: 1996.

Sample PA, Johnson CA. Functional assessment of glaucoma. J Glaucoma 2001;10:S49–52. [PubMed: 11890275]

Schuman JS, Hee MR, Puliafito CA, et al. Quantification of nerve fiber layer thickness in normal and glaucomatous eyes using optical coherence tomography. Arch Ophthalmol 1995;113:586–596. [PubMed: 7748128]

Schuman, JS.; Puliafito, CA.; Fujimoto, JG. Optical coherence tomography of ocular diseases. Slack, Inc; Thorofare, NJ: 2004.

Sihota R, Sony P, Gupta V, Dada T, Singh R. Diagnostic capability of optical coherence tomography in evaluating the degree of glaucomatous retinal nervefiber damage. Invest Ophthalmol Vis Sci 2006;47:2006–2010. [PubMed: 16639009]

Spaeth GL, Lopes JF, Junk AK, Grigorian AP, Henderer J. Systems for staging the amount of optic nerve damage in glaucoma: a critical review and new material. Surv Ophthalmol 2006;51:293–315. [PubMed: 16818081]

Stein DM, Wollstein G, Schuman JS. Imaging in glaucoma. Ophthalmol Clin North Am 2004;17:33–52. [PubMed: 15102512]

Swanson WH, Felius J, Pan F. Perimetric defects and ganglion cell damage: Interpreting linear relations using a two-stage neural model. Invest Ophthalmol Vis Sci 2004;45:466–472. [PubMed: 14744886]

van Velthoven ME, Faber DJ, Verbraak FD, van Leeuwen TG, de Smet MD. Recent developments in optical coherence tomography for imaging the retina. Prog Retin Eye Res 2007;6:57–77. [PubMed: 17158086]

Weber J, Dannheim F, Dannheim D. The topographical relationship betweenoptic disc and visual field in glaucoma. Acta Ophthalmol (Copenh) 1990;68:568–574. [PubMed: 2275353]

Weinreb, RN.; Anton-Lopez, A. Glaucoma definition and classification. In: Easty, DL.; Sparrow, JM., editors. Oxford Textbook of Ophthalmology. New York: Oxford University Press; 1999. p. 642-646.

Wirtschafter JD, Becker WL, Howe JB, Younge BR. Glaucoma visual field analysis by computed profile of nerve fiberfunction in optic disc sectors. Ophthalmol 1982;89:255–267.

Wise, GN.; Dollery, CT.; Henkind, P. The Retinal Circulation. Harper & Row, Publishers, Inc; New York: 1971.

Yamagishi N, Anton A, Sample PA. Mapping structural damage of the optic disk to visual field defect in glaucoma. Am J Ophthalmol 1997;123:667–676. [PubMed: 9152072]

Zangwill LM, Williams J, Berry CC, Knauer S, Weinreb RN. A comparison of optical coherence tomography and retinal nerve fiber layer photography for detection of nerve fiber layer damage in glaucoma. Ophthalmol 2000;107:1309–1315.

Abbreviations

**BVs**

blood vessels

OCT

optical coherence tomography

ONH

optic nerve head

RNFL

retinal nerve fiber layer

SAP

static automated perimetry

A.

B.
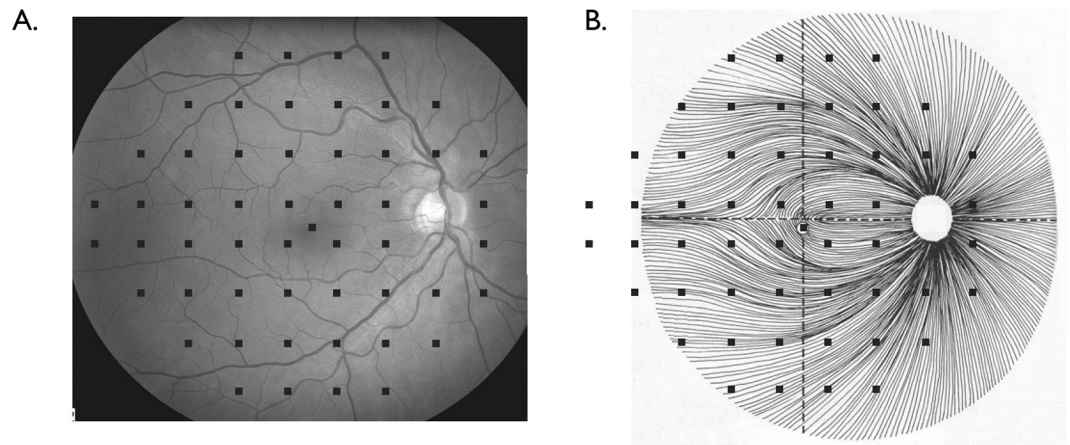
Fig. 1.
(A) A fundus photo of a right eye with the test points for the 24-2 SAP field superimposed.
(B) An artist's sketch of the course of the RGC axons in the retina with the test points for the
24-2 SAP field superimposed.

A.

27 dB

C.

-2 dB = 0.2 log units less sensitive
than age-matched control group

B.
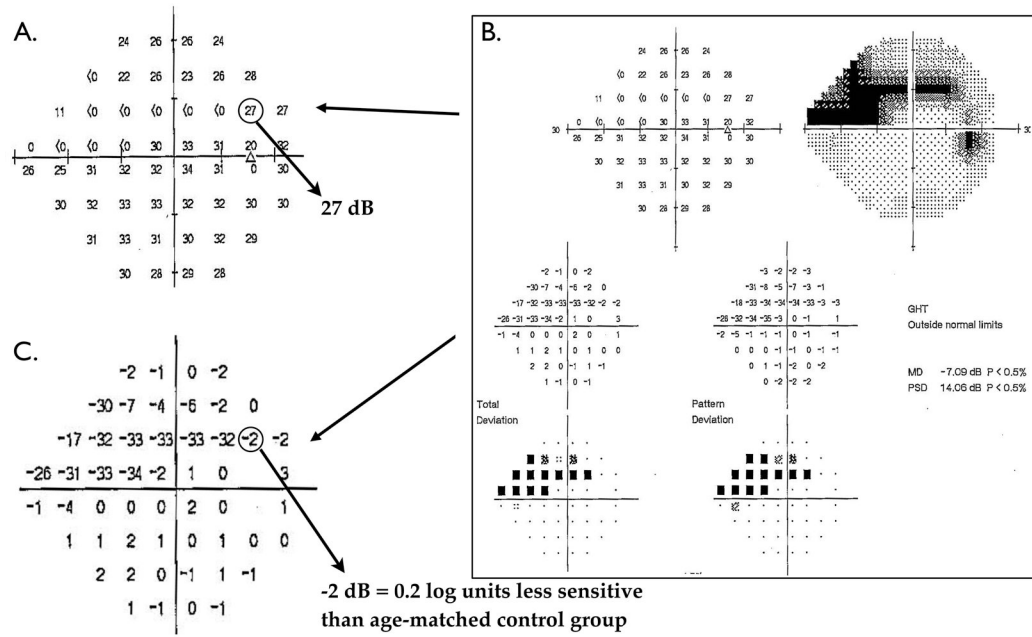
Fig. 2.
The sensitivity (A) and the total deviation (C) plots of a 24-2 SAP test report (B) from an eye
with glaucomatous damage in the superior arcuate region.
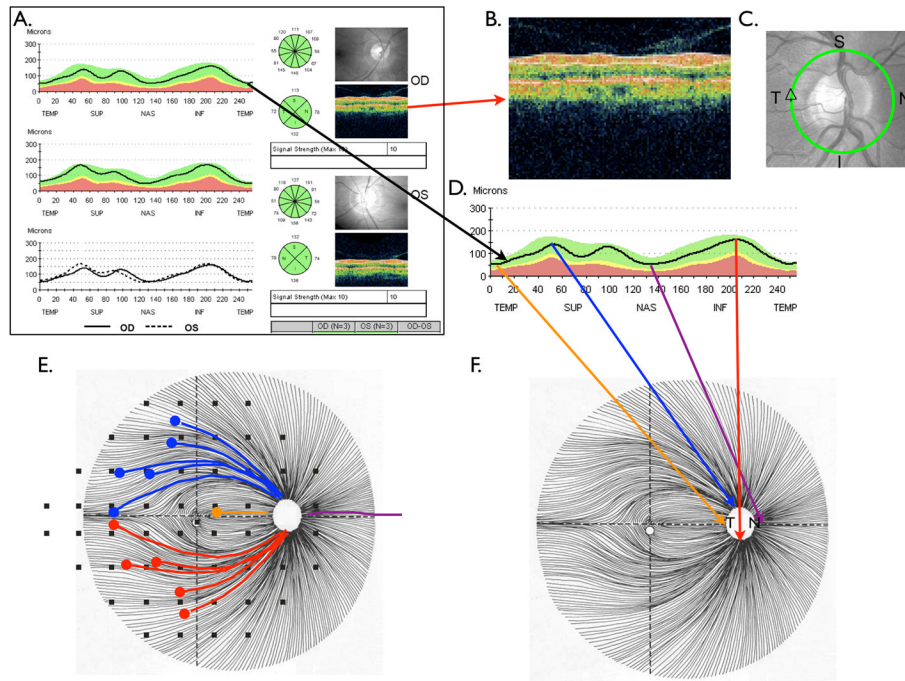
Fig. 3.
(A) A portion of an OCT RNFL thickness report from a commercial machine shown with the pseudo-color scan (B), the scanning circle depicted in green, (C), and the RNFL profile, seen as black line in (D). (E) The approximate locations of the upper (blue) and lower arcuate (red) band of RGC axons. (F) The approximate locations on the RNFL profile are shown related to the corresponding locations around the disc.
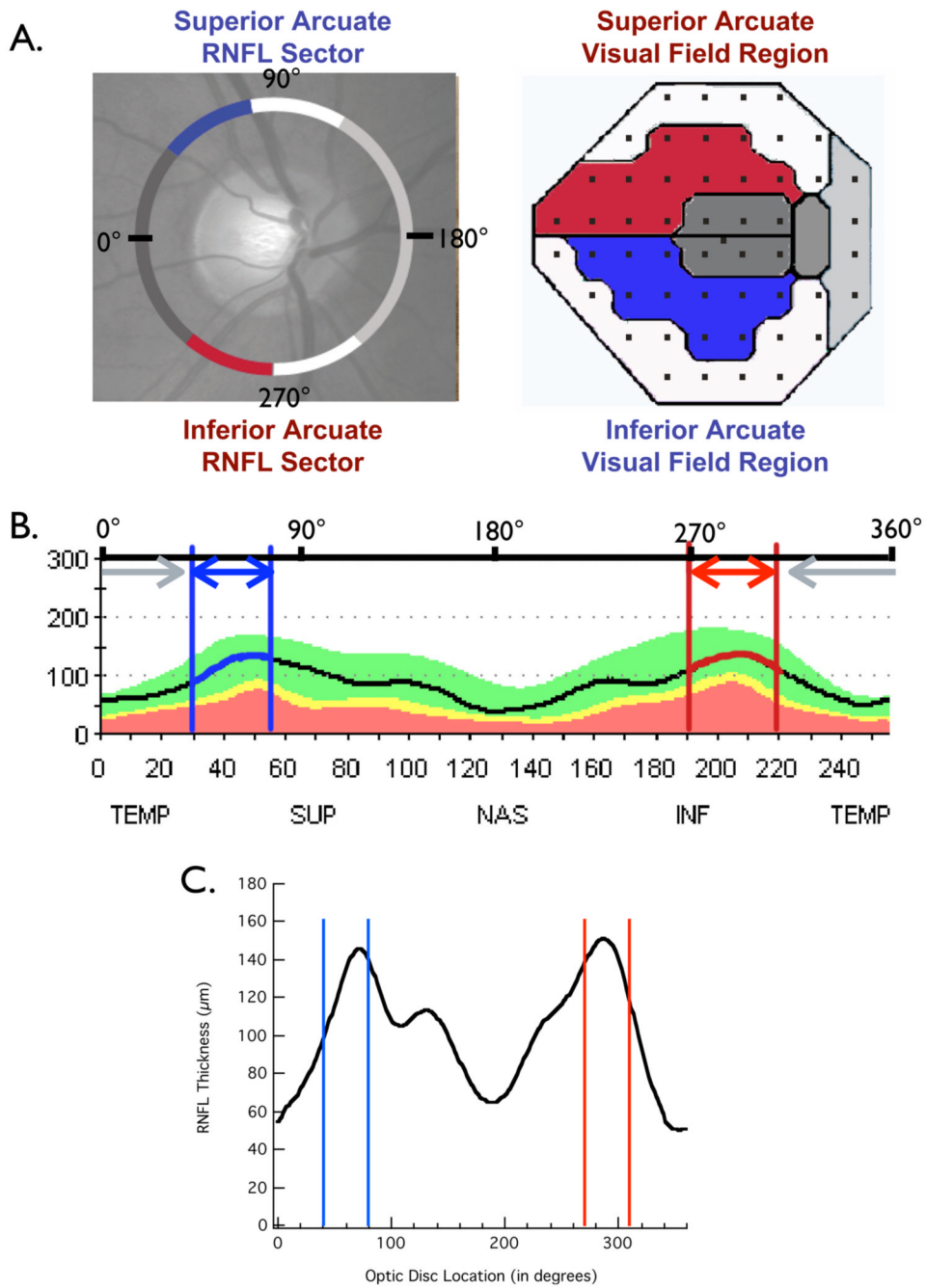
Fig. 4.
(A) Garway-Heath et al. (2000) map relating regions of the visual field to sectors around the disc. (B) The regions of the RNFL profile that correspond to the superior (blue) and inferior (red) temporal arcuate sectors of the disc. (C) The average RNFL profile for 50 normal controls.
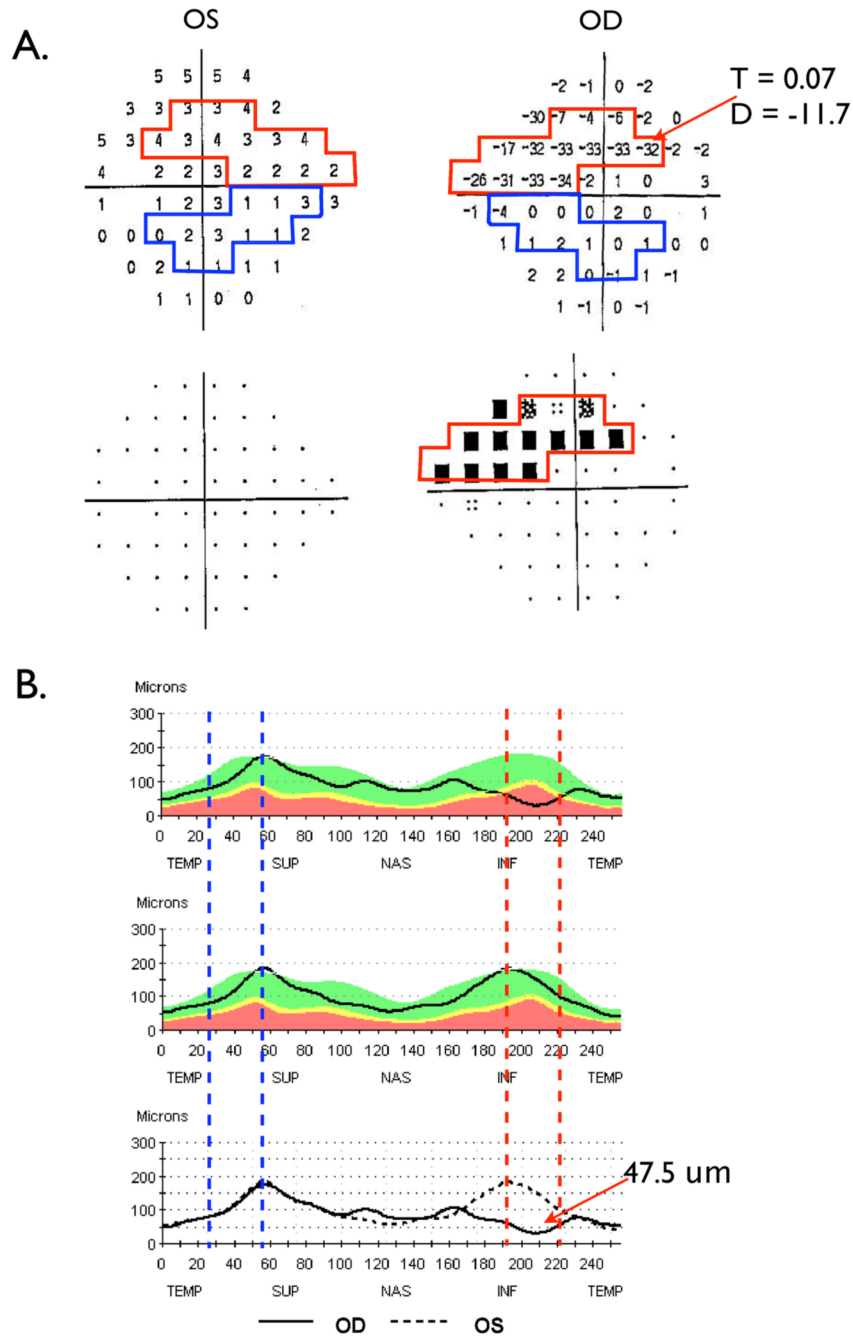
Fig. 5.
(A) Sample total deviations and associated probability plots for a 24-2 SAP field test of a patient with glaucoma. The areas enclosed by the red or blue boundaries signify those visual field test locations associated with the inferior and superior arcuate RNFL bundles, respectively. (B) OCT RNFL profiles for the same patient. The vertical dashed pairs of blue and red lines depict the locations of the RNFL scan that map to the arcuate region of the field shown in (A). Note the loss of RNFL thickness in the inferior arcuate sector of the right eye, corresponding to the superior arcuate field loss, as shown in (A), in the same eye.

normal ganglion cells   **no ganglion cells**

visual field loss 0 dB   **visual field loss -30 dB**

average loss in dB is -15 dB or about 1/ 30 of normal
versus
average loss if antilogged first is about -3 dB or 1/2 of normal
[(1 + 0.001)/2 equals about 1/2]
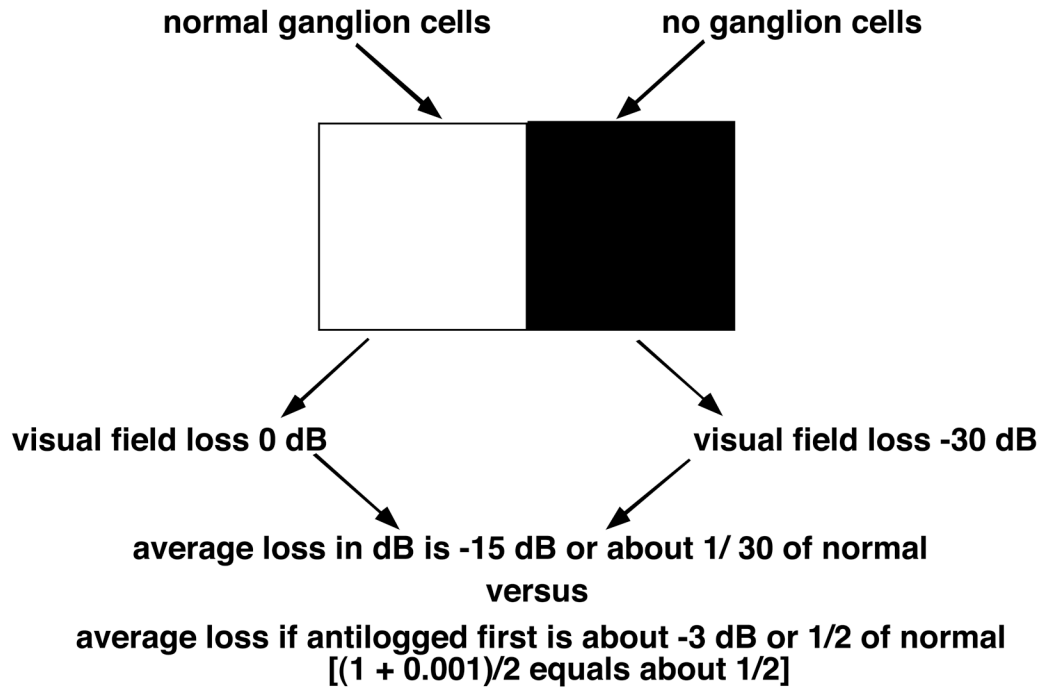
Fig. 6.
An illustration showing why the 24-2 SAP total deviation values are anti-logged before averaging. In the extreme case of a normal region or location (white square) and an adjacent region of complete sensitivity loss (black square), the average calculated field loss for the two areas combined is inaccurate if the values of sensitivity are not first anti-logged before averaging.
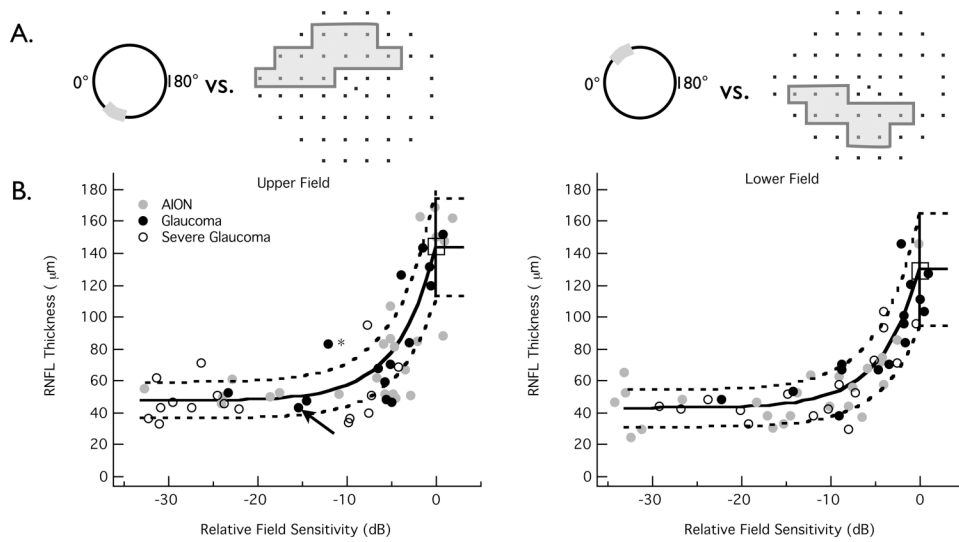
Fig. 7.
(A) A schematic illustrating the location of the corresponding disc sectors and field regions for the superior arcuate field (left panel) and inferior arcuate field (right panel). (B) RNFL thickness as a function of field loss for the upper field/inferior disc (left panel) and the lower field/superior disc (right panel). Data are shown for patients with AION (n=24; filled gray), asymmetric glaucoma (n=15; filled black), and severe glaucoma (n=16; open symbols), and for the mean of a group of 60 age-similar controls (open square). The theoretical curves are eq. 2 fitted by setting $(s_o + b)$ equal to the control value and b equal to one-third this value [i.e. $b=0.33(s_o + b)$]. For the three theoretical curves (50th percentile, 95th percentile, and 5th percentile) in the left panel, $(s_o + b)$ was equal to 173.1, 142.0, and 111.0 μm, and for the three theoretical curves in the right panel, $(s_o + b)$ was equal to 165.0, 130.5, and 95.9 μm.
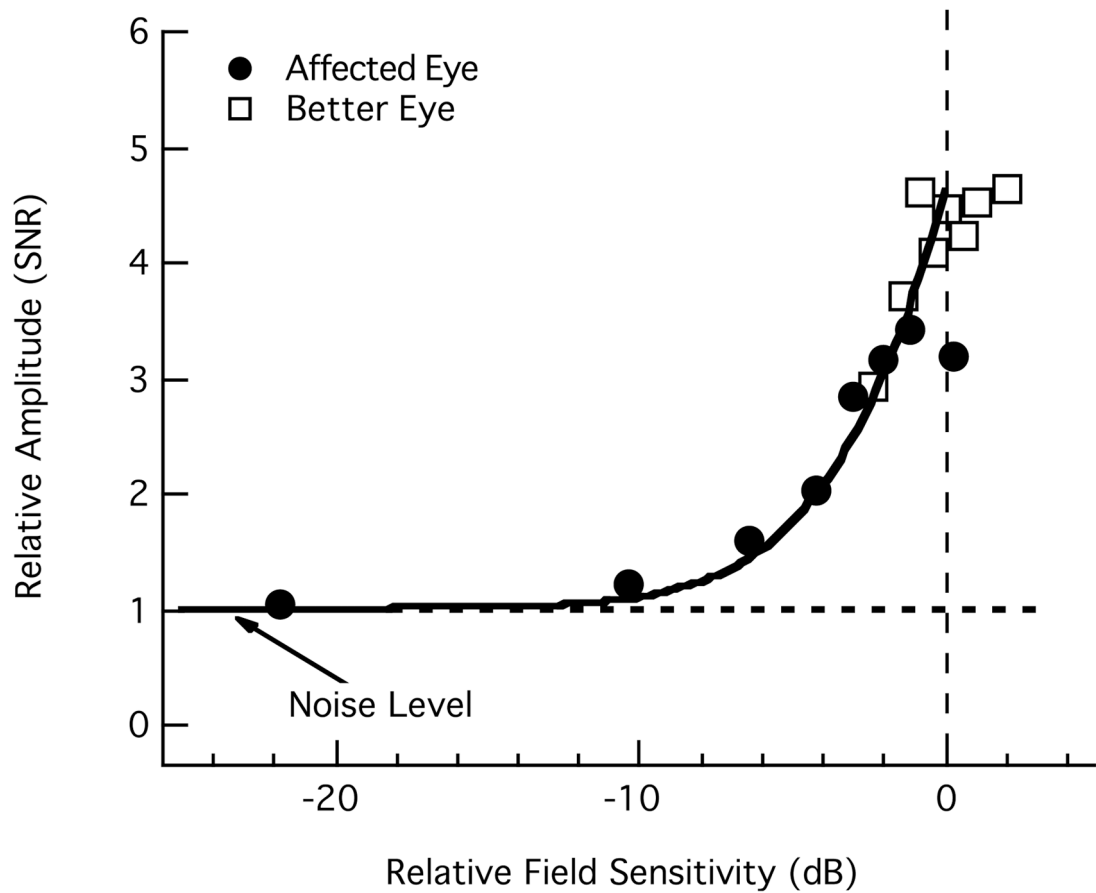
Fig. 8.
The amplitude (signal-to-noise ratio) of a local multifocal visual evoked potential (mfVEP) versus local relative SAP field sensitivity is shown for the mean results for the better (open symbols) and affected (filled symbols) of 20 patients (10 glaucoma and 10 AION) with asymmetrical damage. The smooth curve is the fit of a linear model. Modified from Hood et al (2002).
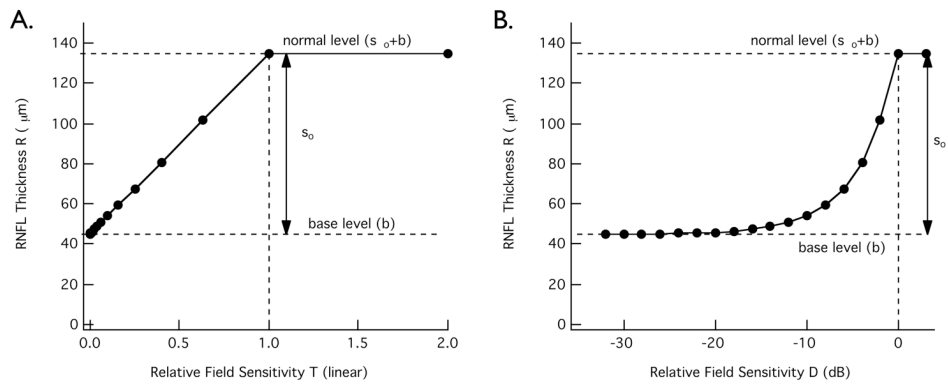
Fig. 9.
The linear model's predicted change in RNFL thickness with changes in SAP field loss express on linear-linear (A) and log-linear (B) coordinates.
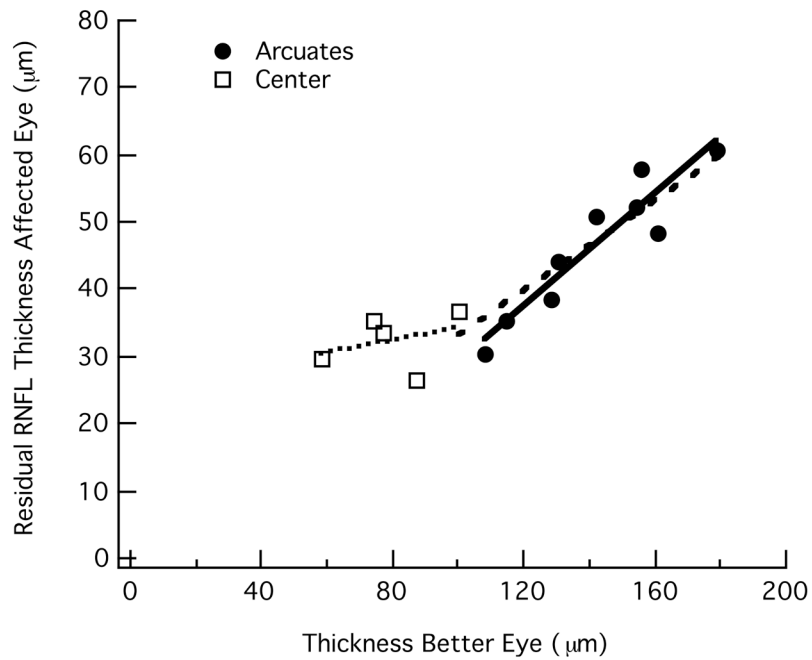
Fig. 10.
Residual RNFL thickness, b, for 9 patients with unilateral AION shown as a function of the RNFL thickness of the corresponding region of the other (unaffected) eye for the upper and lower arcuate field regions (filled symbols) and center (open symbols) of the field. For the filled symbols, the solid line is the best fitting line; the residual thickness is about 1/3 (33%) of the initial/healthy thickness $(s_o + b)$, as indicated by the dashed line. For the open symbols, the dotted line is the line of best fit, $b = 25.3 + 0.088(s_o + b)$.
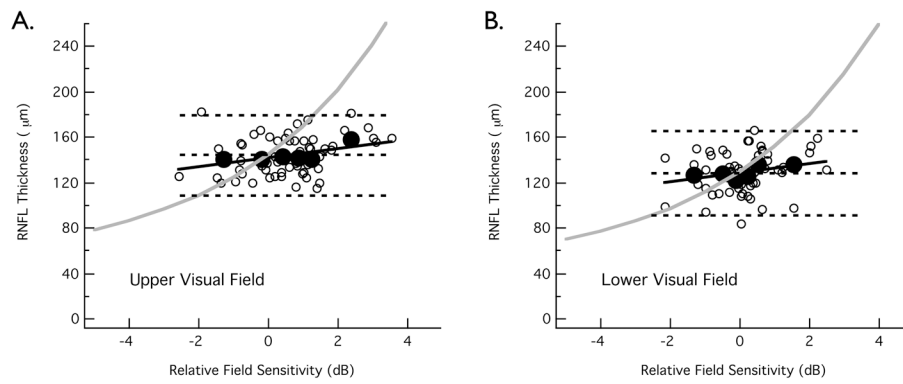
Fig. 11.
RNFL thickness as a function of threshold deviation from age-matched normal eyes for the upper field/inferior disc (A) and lower field/upper disc (B). Open symbols are the results for 60 normal eyes and filled symbols the mean of these data grouped into bins of size 10 after rank ordering them base upon field loss. The dashed lines show the mean and 95% confidence intervals (CI) and the solid the best fitting line to all 60 data points. The gray curve is the same function (eq. 3a) as in Fig. 7B, extended here for values of relative sensitivity greater than 0 dB.
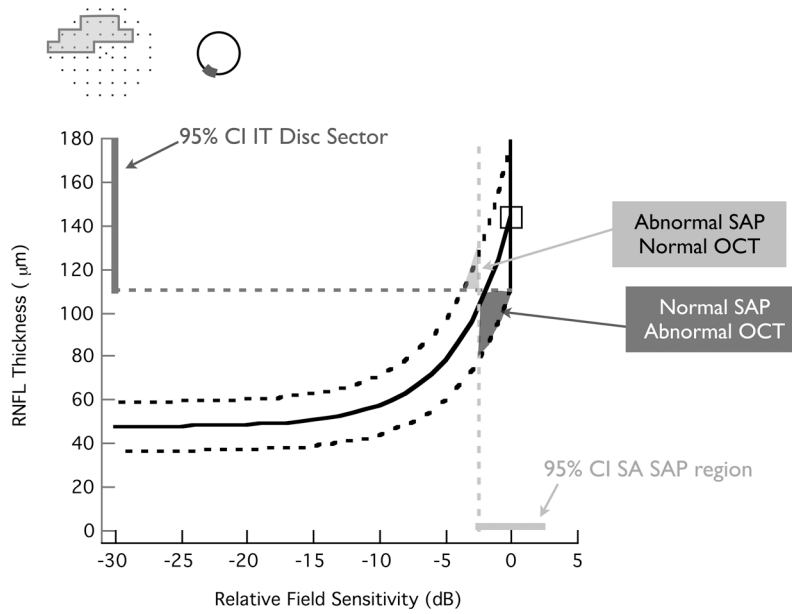
Fig. 12.
Estimating the relative sensitivity of two tests. The theoretical function (dashed and solid curves) relating two tests (RNFL thickness and SAP visual fields) plus an estimation of the variation among normal controls (95% CI), allows the estimation of the relative sensitivity (ratio of gray areas) of two tests. The 95% CI for the OCT comes from Fig. 11 and the 95% CI for the SAP region is 0±1.96SD, where SD is the standard deviation of the SAP total deviation losses for 60 age-matched controls. See text for details.
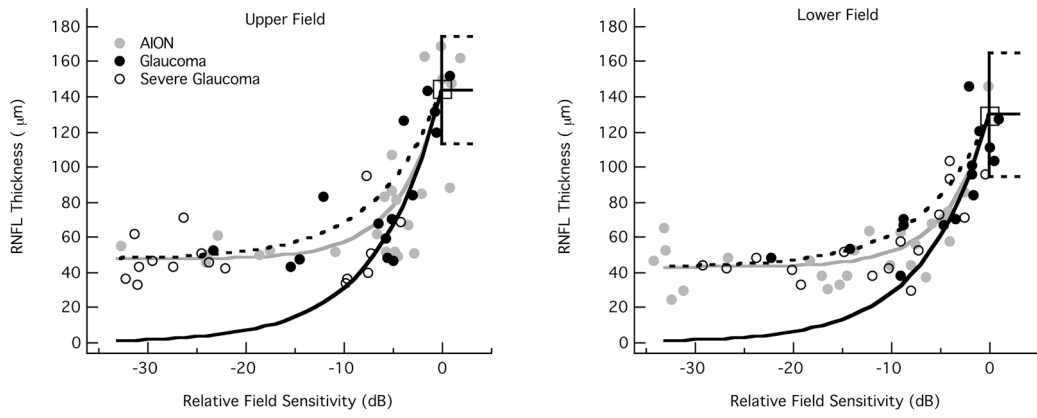
Fig. 13.
Same data as in Fig. 7B with theoretical curves (solid and dashed black) based upon work by
Harwerth et al (2007). See text for details.
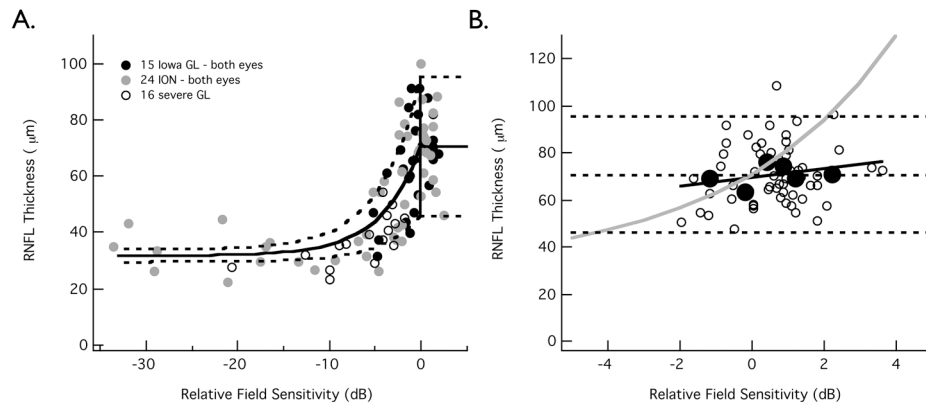
Fig. 14.
(A) RNFL thickness as a function of field loss for the papillomacular bundle (center gray region in Fig. 4A) for the same patients as in Fig. 7B. Data are shown for patients with AION (n=48 eyes; filled gray), asymmetric glaucoma (n=30 eyes; filled black), and severe glaucoma (n=16 eyes; open symbols). The theoretical curves are eq. 3a,b fitted by setting $(s_o + b)$ equal to the control value and b, based upon Fig. 10, equal to $25.3 + 0.088(s_o + b)$. For the three theoretical curves, $(s_o + b)$ was equal to 95.1, 70.4, and 45.7 μm. (B) RNFL thickness as a function of threshold deviation from age-matched normal eyes for the papillomacular bundle (center gray region in Fig. 4A) for the same 60 controls as in Fig. 11. The dashed lines show the mean and 95% confidence intervals (CI) and the solid the best fitting line to all 60 data points. The gray curve is the same function (eq. 3a) as in panel A, extended here for values of relative sensitivity greater than 0 dB.
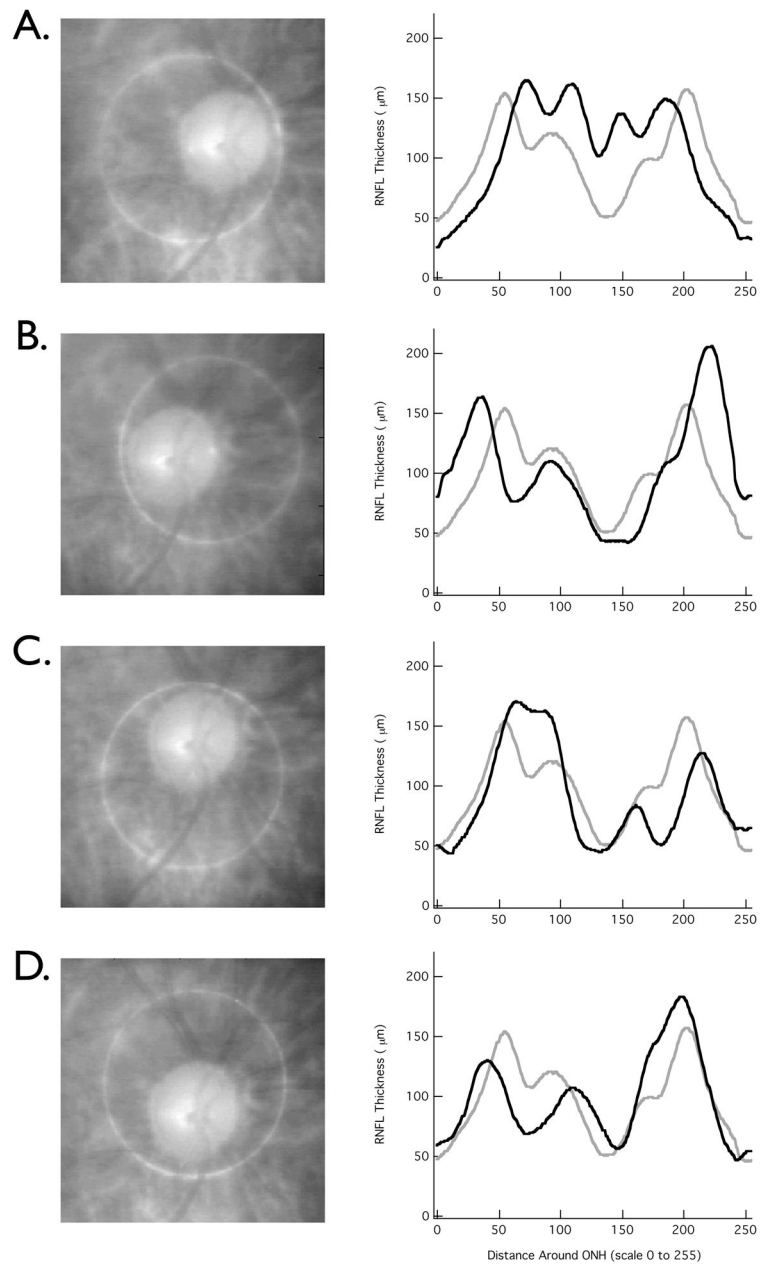
Fig. 15.
The right eye of a normal control was misaligned with respect to the circular scan line so that the disc was off center. The black curve is the RNFL profile for the misaligned circular scan, while the gray curve is the RNFL profile when the circular scan was properly centered on the disc. The profiles change in predictable and systematic ways. (A) Disc right of center: the peaks shift in the nasal direction. (B) Disc left of center: the peaks shift in the temporal direction. (C) Disc above center: the superior peaks increase and inferior peaks decrease in amplitude. (D) Disc below center: the inferior peaks increase and superior peaks decrease in amplitude.
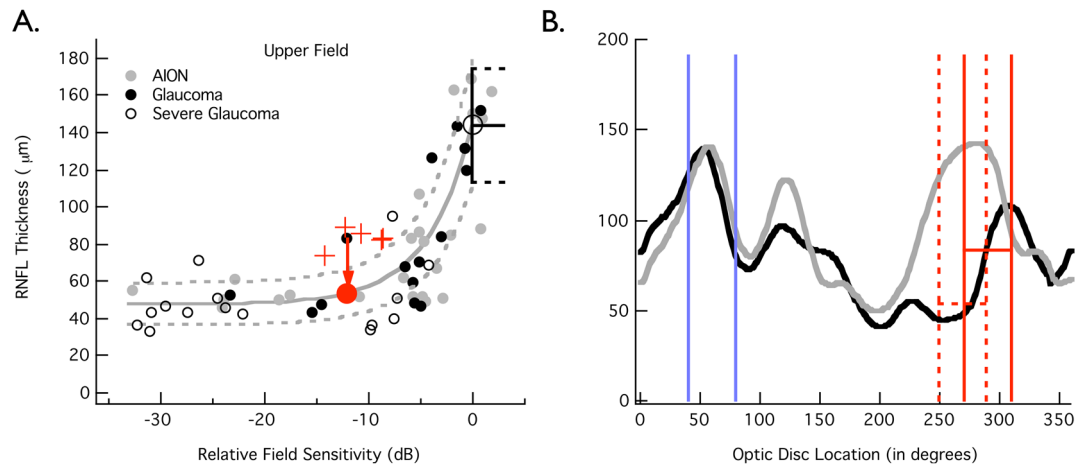
Fig. 16.
(A) The same graph as in Fig. 7B(left panel) with the 5 measurements (red +) for the outlier indicated by the asterisk in Fig. 7B. Note that all repeat measurements were still outlier points (B) The average RNFL thickness for the better (gray line profile) and affected (black line profile) eye of this patient. The solid red and blue lines show the boundaries of the Garway-Heath et al. arcuate regions (see Fig. 4A) and the dashed red lines indicate the shift needed to bring the outlier onto the theoretical curve (the filled red symbol in Fig. 16A).
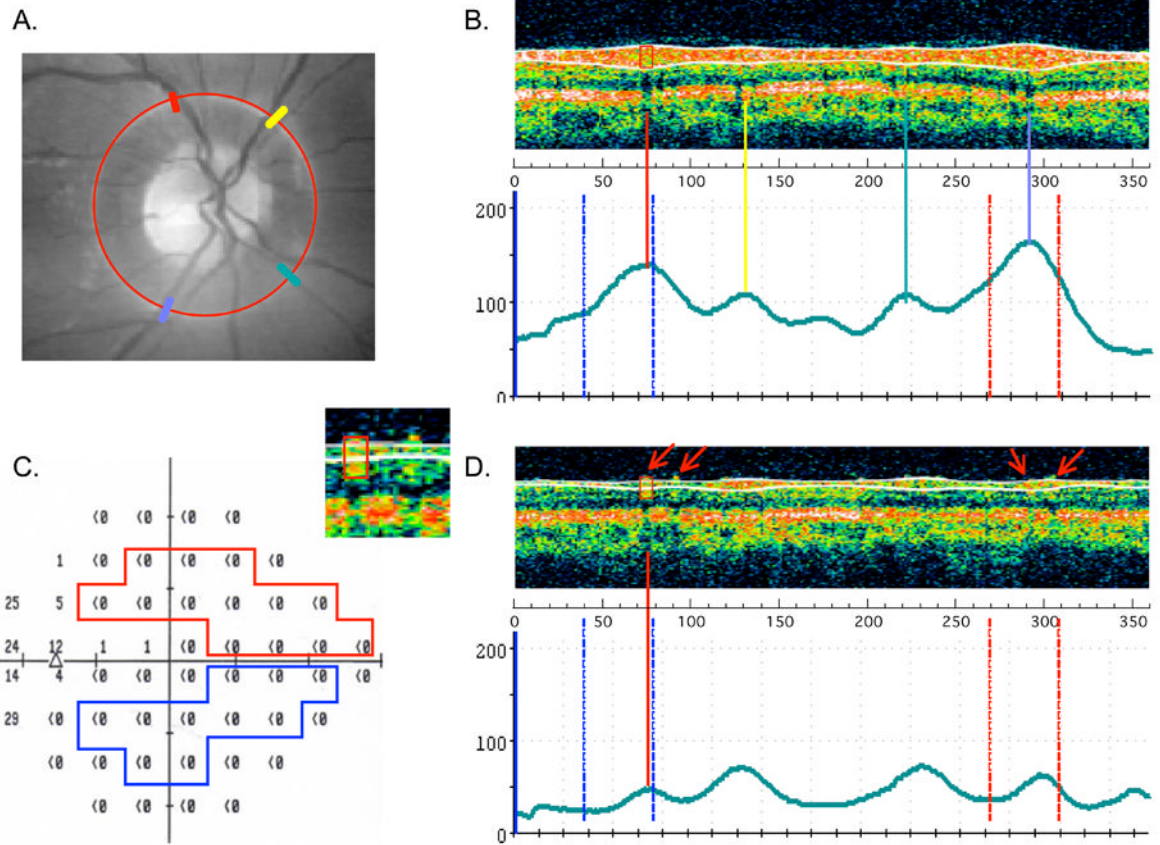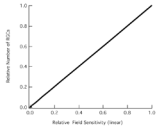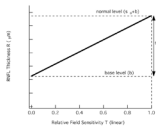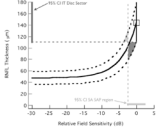
Fig. 17.
Results from patient with unilateral AION illustrating the effects of blood vessels on the OCT
RNFL profile. (A) The disc image of the unaffected right eye showing the location of the peaks
in the RNFL profile in the lower panel of (B). (B) A single scan and the associated RNFL
profile of the unaffected eye. Note that the location of the major and minor maxima of the
RNFL correspond to the location of the major arterial blood vessels, which cause a vertical
linear shadow or dark strip in their locations of the B-scan. (C) The total deviation plot for the
24-2 SAP of the affected left eye. (D) A single scan and the associated thinned RNFL profile
of the affected eye. The arrows indicate the locations of 4 blood vessels, which appear to
contribute to the residual thickness where they are located (red arrows).

A. Possible meanings of ' Does structure precede function?'

RGC   Structural Test

Relational   Statistical   Relational   Statistical

1. Is the relationship between SAP loss and RGC loss non-monotonic?

2. Does a statistically significant RGC loss precede a significant SAP loss?

3. Is the relationship between SAP loss and loss on structural test non-monotonic?

4. Does a statistically significant structural damage precede a significant SAP loss.

B. Our model

Relational   Statistical   Relational   Statistical

Implies that the relationship between SAP loss and RGC loss is linear.

Agnostic.

The relationship between SAP loss (linear scale) and OCT RNFL thickness is linear.

Which is detected first will depend upon SD of tests and conditions involved. Model plus SD predicts which test is more sensitive.

Fig. 18.
A schematic showing 4 possible meanings of the question 'Does structure precede function.?' (A) and how the model presented in Section 4 answers these questions (B).